RSC Pharmaceutics

ROYAL SOCIETY OF CHEMISTRY

REVIEW

View Article Online
View Journal | View Issue

Cite this: *RSC Pharm.*, 2026, **3**, 276

Recent advances in electrospun nanofiber-based implantable drug delivery systems for breast cancer therapy

Jia Xing,[a] Jingjing Feng,[a] Qilin Wang,[a] Deng-guang Yu *[a] and Sim-Wan Annie Bligh*[b]

Breast cancer (BC) remains the most prevalent malignant tumor among women worldwide. While surgical resection currently serves as one of the primary treatment modalities for BC, traditional surgical approaches face challenges including local recurrence, suboptimal prognosis, and systemic side effects of drug administration. Researchers have recently developed implantable drug delivery systems (IDDS) based on electrospun nanofibers for postoperative BC treatment. These electrospun nanofibers exhibit high porosity and specific surface area, which not only enhance contact area with cancer cells but also enable sustained and controlled drug release at targeted sites. This article provides a concise overview of current BC treatment strategies and electrospinning technology, while systematically reviewing recent studies on electrospun nanofiber-based IDDS for BC therapy. The classification is presented from two perspectives: categorization based on the source of loaded drugs (natural compounds, chemotherapeutic agents, *etc.*) and classification according to the stimuli type of smart-responsive IDDS (pH-, magnetic-, light-, or electric-triggered systems). Finally, the paper discusses existing challenges in electrospun nanofiber IDDS for BC treatment and proposes future development directions from multiple aspects, including material optimization, intelligent control systems, and clinical translation considerations.

Received 25th September 2025,
Accepted 20th December 2025

DOI: 10.1039/d5pm00265f

rsc.li/RSCPharma

1. Introduction

Breast cancer (BC) remains one of the most prevalent and lethal malignancies among women globally. According to projected 2025 global cancer statistics, BC is anticipated to rank first in new cancer diagnoses among women, accounting for 32% of cases, while also holding the second position in cancer-related mortality, representing 14% of female cancer deaths.[1] BC arises from the malignant transformation of mammary gland cells in breast tissue. In its earliest *in situ* form, the disease is non-life-threatening and detectable at preliminary stages. However, cancerous cells exhibit invasive behavior, penetrating adjacent tissues and potentially developing into tumors.[2] Critically, once cancer cells metastasize to regional lymph nodes, they demonstrate a high propensity for systemic dissemination to distant organs, inducing secondary oncogenic pathologies that directly compromise survival.[3,4]

Current treatment strategies for BC are tailored based on patient-specific factors, tumor subtype, and metastatic progression, with primary modalities including chemotherapy, radiotherapy, targeted therapy, immunotherapy, and surgical intervention.[5] Compared to other approaches, surgical resection offers distinct advantages: it significantly reduces treatment duration, synergizes with adjuvant therapies to eliminate residual cancer cells, and achieves maximal local control of primary tumors and regional lymph nodes through complete excision of malignant lesions.[6–8] However, despite these benefits, surgical treatment carries inherent limitations, including risks of locoregional recurrence and distant metastasis post-operation, which contribute to suboptimal long-term prognosis in BC patients.

With advancements in therapeutic technologies, researchers have identified that localized drug delivery systems can significantly enhance effective drug concentrations at tumor sites, prolong drug-tumor contact duration, and enable drug penetration to regions inaccessible *via* conventional systemic administration. Critically, this approach mitigates systemic toxicity associated with postoperative chemotherapy and reduces risks of metastatic recurrence. By fulfilling the dual requirements of high-dose short-term delivery and sustained low-dose maintenance, implantable drug delivery devices positioned within the tumor cavity offer a strategic solution to control cancer cell proliferation while improving anticancer efficacy.[9–11]

[a]*School of Materials and Chemistry, University of Shanghai for Science and Technology, Shanghai 200093, China. E-mail: ydg017@usst.edu.cn*
[b]*School of Health Sciences, Saint Francis University, Hong Kong 999077, China. E-mail: abligh@sfu.edu.hk*

The limitations inherent in conventional therapeutic regimens have prompted investigations into integrating nanotechnology with implantable drug delivery systems (IDDS) for enhanced precision in BC treatment.[12] As presented in Table 1, carrier systems such as nanoparticles, liposomes, micelles, hydrogels, and polymeric nanospheres possess unique features and show great potential in BC therapy. However, they also face respective challenges, including *in vivo* stability, targeting efficiency, scalable production, and clinical translation.[13–18] Among the multitude of investigated approaches, nanofibers have emerged as a particularly promising platform for post-operative adjuvant therapy of BC. Their distinctive advantages stem from the local implantable drug delivery modality, high flexibility in drug loading, and excellent tunability of drug release profiles. Fig. 1 illustrates (A) various nanocarriers applied in BC therapy along with the operational process of a nanofiber-based IDDS, and (B) three suggested routes for promoting the commercialization of nano products created in laboratories.

The selection of nanofiber fabrication techniques plays a decisive role in determining their performance as drug carriers, as key physical parameters—including diameter, porosity, and mechanical properties—directly influence their functionality. A range of methodologies have been developed in this field, such as self-assembly, phase separation, template synthesis, solution blow spinning, and electrospinning. Among them, self-assembly enables molecular-level structural precision but is time-consuming;[41] phase separation and template methods each offer advantages in fabricating specific three-dimensional architectures or fibers with uniform diameters, though both are constrained by limited scalability;[42,43] solution blow spinning operates without a high-voltage electric field and provides high production efficiency, yet typically yields fibers with broad diameter distribution and less defined morphological control.[44,45] Among these approaches, electrospinning has emerged as the predominant technique for constructing localized IDDS, owing to its material versatility, flexible drug-loading capacity, tunable fiber morphology, and strong compatibility with modern controlled-release strategies.[46–48] This has further spurred numerous methodological innovations oriented toward clinical translation.[49–52]

Electrospun nanofiber-based IDDS have emerged as a transformative approach for localized post-surgical BC treatment. By incorporating diverse therapeutic agents—such as natural compounds, chemotherapeutic drugs, or multidrug combinations-into the nanofiber matrix, these systems enable targeted therapy tailored to specific tumor biology. Beyond conventional drug delivery, electrospun nanofiber IDDS demonstrate remarkable multifunctionality through integration with complementary treatment modalities.[53–55] A prominent example is their design as stimuli-responsive drug delivery systems (SRDDS), which synergize with chemotherapy, thermotherapy, or other approaches to introduce intelligent, context-aware therapeutic strategies for BC management. SRDDS are engineered by incorporating stimuli-responsive biomaterials into nanofiber architectures. These materials must exhibit biocompatibility and the ability to trigger on-demand drug release in response to internal (*e.g.*, pH, enzyme levels) or external (*e.g.*, light, magnetic field) stimuli post-implantation. This "on-demand" release mechanism achieves spatiotemporal control

Table 1 Comparison of primary nanocarriers for BC treatment

Carrier type	Core advantages	Primary limitations	Potential applications & challenges in BC treatment
Nanoparticles (*e.g.*, AuNPs, AgNPs)	• Unique optical/electrical/thermal properties for theranostics[19]	• Rapid immune clearance[22]	Used in photothermal therapy and image-guided chemotherapy; key challenges are improving targeting and prolonged circulation
	• Easy surface functionalization to improve targeting[20,21]	• Potential long-term toxicity concerns[22]	
Liposomes	• Core–shell structure enhances solubility of poorly soluble drugs[23]	• Specific side effects (*e.g.*, hand-foot syndrome)[25]	Classical carriers for chemotherapy; focus on managing side effects and scalable production for clinical translation
	• Can be designed as stimuli-responsive systems using EPR effect[24]	• Complex preparation and poor storage stability[25]	
Polymeric micelles	• Enable complex, multi-stage drug release systems[26]	• Limited *in vivo* stability, may dissociate prematurely[27]	Accumulate in tumors *via* EPR effect; need improved stability and tumor penetration
	• Allow temporal control of multi-drug release[26]	• Mostly in preclinical stage[28]	
Hydrogels	• Extend drug half-life with controlled release[29]	• High synthesis cost, difficult to scale up[31]	Local implantable platforms for post-surgery therapy; reliable *in vivo* validation needed
	• Smart responsiveness for on-demand release[30]	• Poor simulation of real *in vivo* microenvironment[32]	
Polymeric nanospheres	• Biodegradable with good *in vivo* safety[33]	• Susceptible to immune clearance[36]	Enable sustained release with reduced side effects; need to overcome physiological barriers and improve targeting
	• Precise control of drug release kinetics[34,35]	• Limited targeting and barrier penetration[36]	
Nanofibers	• High surface area/porosity for efficient drug loading[37]	• Localized rather than systemic application[39]	High potential for local therapy in post-surgical BC cavities; main focus of this review
	• Ideal for local implantation and long-term combination therapy[38]	• Challenges in GMP scale-up and quality control[40]	

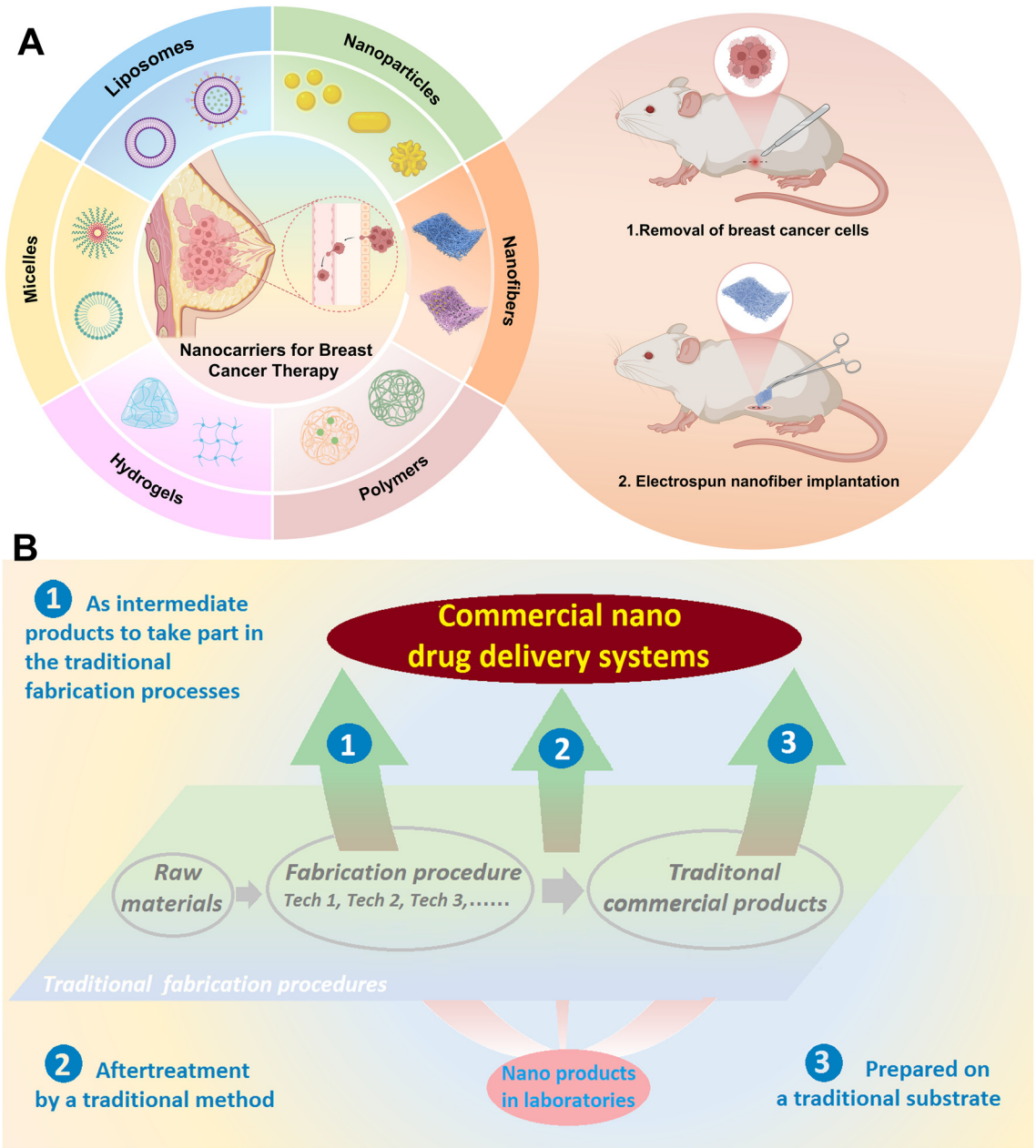

Fig. 1 A. Schematic illustration of various nanocarriers applied in BC therapy and the application process of the nanofiber-based IDDS; B. three suggested routes for promoting the commercialization of nano products created in laboratories. Reproduced from ref. 18 with permission from Bentham, copyright 2026.[18]

over drug administration, optimizing dosage precision, spatial localization, and temporal regulation.[56–58] Compared to systemic drug delivery, SRDDS based on electrospun nanofibers implanted at the lesion site offer unique advantages: localized drug action responsive to tumor microenvironment cues, minimized systemic toxicity, and enhanced therapeutic efficacy through controlled release kinetics.

This article briefly outlines the current landscape of BC treatment and the fundamentals of electrospinning technology, while systematically summarizing the advantages of electrospun nanofiber-based IDDS in BC therapy. A focused review is presented on recent research advances in electrospun nanofiber IDDS for post-surgical BC management, categorizing these studies along two key dimensions: the classification is presented from two perspectives: categorization based on the source of loaded drugs (natural compounds, chemotherapeutic agents, *etc.*) and classification according to the stimuli type of smart-responsive IDDS (pH-, magnetic-, light-, or electric-triggered systems). Finally, the paper discusses existing challenges in electrospun nanofiber IDDS for BC treatment and proposes future development directions from multiple aspects, including material optimization, intelligent control systems, and clinical translation considerations.

2. Electrospinning

2.1. Introduction to electrospinning

Electrospinning, a branch of electrohydrodynamics, employs a "top-down" fabrication approach to produce micro- to nanoscale fibers from various polymers under high-voltage conditions. This process allows for the incorporation of functional additives, surfactants, and crosslinking agents to tailor fiber properties.[59,60] Due to its operational simplicity, cost-effectiveness, and broad material compatibility, electrospinning has become a cornerstone technique for nanofiber fabrication.[60,61] The commercialization of electrospinning dates to 1944, when Anton Formhals patented and refined the technology for textile yarn production.[62] Subsequent decades saw its adaptation for applications such as wound dressings and air filtration membranes. By the 1990s, research groups led by Darrell Reneker and Gregory Rutledge revitalized the field, establishing electrospinning as a focal point of nanomaterials research.[63,64] Since then, electrospinning has evolved from single-component systems to multifunctional composite materials,[65] expanding its applications across diverse fields including biomedical applications, tissue engineering, sensing technologies, food packaging, and energy storage devices.[66–71] Concurrently, advancements in fiber architecture design—such as aligned fiber arrays and hierarchical structures—have unlocked novel functionalities.[72] In recent years, electrospun nanofiber-based DDS have reached a mature stage of development for anticancer therapy, demonstrating significant potential to advance human health through localized, controlled, and targeted therapeutic strategies.

The experimental setup for electrospinning is fundamentally simple, primarily consisting of four components: a high-voltage power supply, a syringe pump, a spinneret, and a fiber collector, as illustrated in Fig. 2. The high-voltage power supply provides an electric field using either direct current (DC) or alternating current (AC),[73,74] with AC electrospinning inducing distinct jet dynamics that result in significantly different fiber morphologies compared to DC-driven processes.[75] During the electrospinning process, critical operational parameters include: applying high voltage to the spinneret to initiate polymer jet formation, precisely regulating the flow rate and velocity of the polymer solution *via* the syringe pump, tailoring the spinneret geometry to control fiber architecture, and grounding the collector to stabilize the electric field for efficient fiber deposition.

The fundamental principle of electrospinning lies in utilizing electrostatic field forces to elongate polymeric fluids into continuous fibers.[76] The process involves the following stages: at room temperature, a polymer solution is extruded from the spinneret *via* a syringe pump. A high-voltage power supply applies an electric potential to the spinneret, inducing charge accumulation within the pendant droplet.[77] When the electric field strength surpasses a critical threshold, the electrostatic repulsion within the droplet overcomes its surface tension, causing the droplet to deform from a sphere into a cone, known as the Taylor cone.[78] Subsequently, a charged jet is ejected from the apex of the Taylor cone, initially propagating linearly before undergoing vigorous whipping instabilities due to bending perturbations. During this stage, solvent evaporation induces rapid solidification of the jet, which is simultaneously stretched to submicron or nanoscale diameters. The solidified fibers are ultimately deposited onto the grounded collector, forming a nonwoven mat with tunable porosity and fiber alignment.[79–81]

The fabrication of nanofibers *via* electrospinning is influenced by three primary parameter categories: system parameters, process parameters, and environmental parameters.[82,83] Fiber diameter control predominantly depends on process parameters, including applied voltage, solution flow rate, and collector distance. The magnitude of

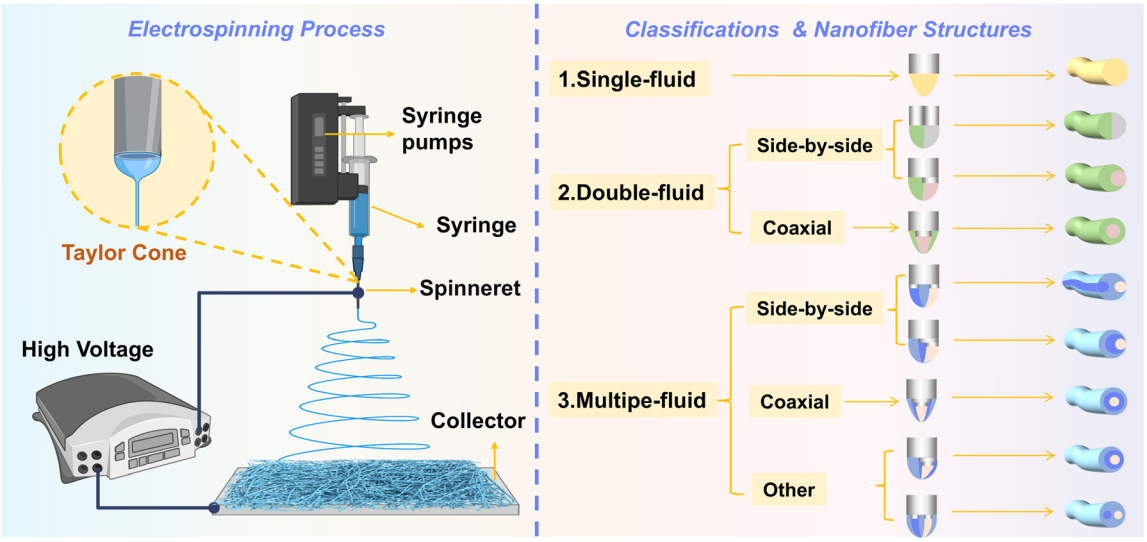

Fig. 2 Principle and process of electrospinning; classification of electrospinning and corresponding nanofiber structures.

the applied voltage determines the charge density carried by the jet, the electrostatic repulsion forces between charges, and the intensity of interactions between the jet and the external electric field.[84] Higher voltages generally promote the formation of finer fibers due to enhanced jet stretching.[85] Conversely, increased flow rates may lead to thicker fiber diameters by delivering a greater volume of solution to the jet.[86] The distance between the spinneret tip and the collector governs the stretching and solidification period prior to fiber deposition, with longer distances typically allowing sufficient solvent evaporation and polymer solidification to achieve uniform fiber morphology.[87]

Through parameter optimization and matrix modification, the morphology, diameter, and alignment of electrospun nanofibers can be precisely tailored to meet application-specific requirements across diverse fields. By selecting various polymeric substrates, loading single or multiple therapeutic agents, and incorporating bioactive additives, electrospun nanofibers serve as advanced DDS for targeted cancer therapy.[52] Strategic material selection and functionalization further enable these fibers to exhibit enhanced biocompatibility, tunable biodegradability, high drug-loading capacity, and stimuli-responsive properties. This allows for subcutaneous implantation of nanofiber-based devices, which deliver localized therapeutic doses with elevated drug concentrations at the tumor site while minimizing systemic toxicity. Specifically, IDDS based on electrospun nanofibers offer a highly viable solution for localized BC therapy, effectively addressing challenges such as postoperative residual cancer cells, metastatic dissemination, and tumor recurrence.

Table 2 Advantages and disadvantages of three electrospinning methods

Classification	Main advantages	Main disadvantages
Single-fluid electrospinning	• Simple process and easy operation • Wide applicability to various polymers • High uniformity of fiber structure	• Limited control over fiber morphology and composition • Potential phase separation between different polymers • Difficult to achieve multi-drug delivery and complex release profiles
Dual-fluid electrospinning	• Capable of fabricating complex architectures (*e.g.*, core–sheath, Janus) • Coaxial structure protects sensitive drugs and enables sustained release • Side-by-side structure facilitates biphasic drug release	• More complex equipment and process than single-fluid • More challenging parameter control, prone to clogging or instability • Side-by-side configuration struggles to achieve slow release
Multi-fluid electrospinning	• Enables construction of sophisticated multi-stage drug control systems • Achieves temporal release of multiple therapeutic agents • Integrates advantages of both coaxial and side-by-side electrospinning	• Extremely complex and difficult fabrication process • Requires precise, cascaded control over all parameters • All polymers and drugs can interact, complicating the process

2.2. Classification of electrospinning

The rapid advancements in electrospinning technology have enabled the transition of nanofiber architectures from monolithic to highly diverse forms, where the incorporation of multi-fluid systems has driven unprecedented structural innovation. Central to this evolution is the design versatility of spinnerets, which enables precise guidance of multiple fluid streams into the electric field for fabricating nanostructured fibers with programmable complexity.[88] Based on the number of fluid phases, electrospinning is categorized into single-fluid, dual-fluid, and multi-fluid modalities. Fibers produced *via* dual- and multi-fluid electrospinning are systematically classified into three principal morphologies: uniaxial, core–shell (or coaxial), and Janus (side-by-side) configurations. Table 2 summarizes the respective advantages and disadvantages of the three electrospinning techniques and Fig. 2 illustrates the categories of fluid-based electrospinning technologies and their corresponding nanofiber structural classifications.

2.2.1. Single-fluid electrospinning. Single-fluid electrospinning, also termed monoaxial electrospinning, produces the simplest fiber architecture. In this process, polymers, model drugs, or biomolecules are directly dissolved in a solvent to form a homogeneous spinning solution, which can be classified as blend electrospinning. While the principle is straightforward, this method imposes stringent requirements on polymer spinnability and necessitates drug solubility in the polymer solution for DDS applications. If the drug exhibits poor solubility in the polymer solution, it tends to phase-separate and accumulate on the fiber surface, leading to an initial burst release of the drug—a significant drawback for DDS that require controlled or sustained release profiles. For drugs and polymers with limited mutual solubility, minor amounts of cosolvents (*e.g.*, dimethyl sulfoxide, DMSO) can be introduced to enhance miscibility.[89] For instance, Park *et al.*[90] demonstrated that incorporating DMSO as a polar cosolvent in a poly (lactic acid) (PLA)/doxorubicin (DOX) system enabled uniform drug internalization within electrospun fibers and improved drug loading efficiency. In another investigation, hemin was successfully encapsulated within polyvinylpyrrolidone (PVP) nanofibers *via* an optimized electrospinning technique. The resulting formulation rapidly dissolved under physiological conditions (PBS, pH 7.4) to form nanoparticles, increasing the solubility of hemin to 273 μM. This represents a remarkable enhancement of over 200-fold, surpassing the efficacy of all known solubilizing agents.[91]

Despite its simplicity, single-fluid electrospinning is restricted to fabricating basic nanofibers with limited functional versatility due to constrained drug-polymer compatibility. In BC therapy, monoaxial electrospun fibers primarily

serve as passive drug depots to induce tumor cell apoptosis, with suboptimal controlled release performance and minimal capacity for multifunctional therapeutic integration.

2.2.2. Dual-fluid electrospinning. Dual-fluid electrospinning encompasses two distinct methodologies: coaxial electrospinning and side-by-side (Janus) electrospinning. Coaxial electrospinning produces core–shell nanofibers, whereas side-by-side electrospinning yields Janus nanofibers with spatially segregated functionalities.

In 2003, Sun *et al.*[92] pioneered the fabrication of core–shell nanofibers using coaxial electrospinning. Core–shell architectures significantly enhance sustained drug release by encapsulating hydrophilic drugs within the core phase, which is shielded by the sheath polymer. This configuration prevents initial burst release through the buffering effect of the outer layer, thereby prolonging therapeutic delivery – a critical advantage for chronic disease management.[93] For instance, Hai *et al.*[94] employed a non-spinnable lipid solution as the sheath fluid and a blend of berberine hydrochloride (BHC) and ethyl cellulose (EC) as the core fluid, achieving sustained BHC release from coaxial nanofibers for the first time. By selecting diverse sheath polymers, researchers can tailor drug release kinetics.[95] Reise *et al.*[96] demonstrated this by utilizing PLA as the protective sheath and metronidazole (MNA) in the core, resulting in prolonged MNA release for localized periodontitis therapy. Similarly, Liu *et al.*[97] engineered core–shell fibers with curcumin (Cur)—a poorly water-soluble drug—encapsulated in a PVP core matrix and a hydrophobic poly(3-hydroxybutyrate-*co*-3-hydroxyvalerate) (PHBV) sheath, effectively delaying Cur release.

In 2003, Gupta *et al.*[98] pioneered the fabrication of Janus (or side-by-side) nanofibers *via* side-by-side electrospinning, a dual-fluid process that simultaneously electrospins two bicomponent polymer solutions. Unlike core–shell structures, Janus nanofibers feature two distinct compartments that directly interface with the surrounding environment. The geometry and interfacial contact area of these compartments can be precisely engineered by modifying the spinneret design, enabling tunable functionalities such as anisotropic mechanical properties or biphasic drug release profiles.[99–101] The advent of side-by-side electrospinning has expanded the utility of dual-fluid systems in cancer therapy. For instance, Zhou *et al.*[102] developed photothermal Janus fibers using a custom-designed eccentric dual-fluid spinneret, which enabled synergistic photothermal–chemotherapeutic combination therapy for hepatocellular carcinoma. Similarly, Kuang *et al.*[103] engineered an implantable sponge-nanofiber Janus scaffold with spatially segregated loads of lyophilized inactivated tumor cells, the immunoadjuvant imiquimod, and 5-fluorouracil (5-FU) for post-surgical immunochemotherapy.

The stable process of coaxial electrospinning commences with the establishment of a compound jet.[104] A fundamental requirement is the immiscibility of the inner and outer fluids, a prerequisite for maintaining separate jet components and achieving the intended core–sheath or Janus morphology; partial miscibility results in a blended interface at the core–sheath boundary. Equally critical is that the two fluids exhibit similar dielectric properties, enabling them to withstand comparable electric field forces and stretch in concert. Ultimately, precise manipulation of the flow rates emerges as the key factor governing the extent of core encapsulation and the final fibrous structure.[105]

Notably, earlier studies assumed that both polymer matrices in coaxial or side-by-side electrospinning must exhibit spinnability.[106] However, recent technological advancements have demonstrated that one fluid in dual-fluid systems can be a diluted polymer solution, surfactant, or even pure solvent.[107] For example, Yu *et al.*[108] employed modified coaxial electrospinning with a sheath fluid comprising only mixed solvents, producing nanofibers with smaller average diameters, enhanced uniformity, and smoother surfaces compared to monoaxial fibers. These fibers also exhibited superior zero-order drug release kinetics. This breakthrough broadens the scope of dual-fluid electrospinning, enabling the design of multifunctional drug-loaded nanofibers with programmable release profiles (sustained or rapid) and expanding material selection to include solvents, solutes, and surfactants.[109,110]

2.2.3. Multi-fluid electrospinning. Building upon the complexity of dual-fluid systems, multi-fluid electrospinning represents a further evolution. Multi-fluid electrospinning, an advanced evolution of dual-fluid electrospinning, utilizes three or more distinct liquid phases to fabricate nanofibers with hierarchical architectures or multi-compartmental functionalities. This technology achieves precise spatial segregation of polymers, drugs, or functional additives within a single fiber, offering unparalleled versatility in material design and application-specific performance optimization. Beyond triaxial coaxial electrospinning and triaxial side-by-side electrospinning, hybrid configurations such as side-by-side electrospinning with coaxial cores and coaxial electrospinning with side-by-side cores have been developed. Critically, only one dominant fluid in the system must exhibit spinnability, while others may be non-spinnable (*e.g.*, solvents, surfactants). Regardless of the number of fluids, the process generates a single Taylor cone, a unified jet, and a shared whipping motion zone during fiber formation.

Compared to single- and dual-fluid electrospinning, multi-fluid systems produce structurally intricate fibers requiring meticulous control over multiple variables. The fundamental prerequisites for multi-fluid electrospinning share commonalities with coaxial processes, yet demand mutual immiscibility between all adjacent fluids and involve more intricate parameter optimization.[88] For instance, the relationship between the total flow rate and applied voltage requires careful consideration. The complex nanostructures can be fabricated through three primary routes: the direct electrospinning of multiple fluids, post-processing of electrospun products, and ingenious design of the composition, constituents, and their spatial distribution. As the number of fluid channels increases, charge repulsion may occur at the interfaces between dissimilar materials, resulting in their separation under the influence of the electric field. For instance, Wang *et al.*[111] engineered a

triaxial core–shell nanorepository *via* modified triaxial electrospinning, featuring an outermost blank coating and an intermediate drug-loaded core–shell layer. This three-layered architecture eliminated initial burst release, prolonged sustained drug release, and minimized late-stage tailing effects compared to conventional coaxial fibers. Similarly, Zhao *et al.*[112] fabricated triple-layered eccentric side-by-side composite fibers using a custom three-channel spinneret. The outermost hydrophilic polymer layer loaded with ketoprofen achieved 50% drug release within 0.37 hours for rapid analgesic and anti-inflammatory effects, while the middle MNA layer provided sustained release, and the innermost nano-hydroxyapatite (HAP) layer directly interfaced with periodontal tissue to promote alveolar bone regeneration.

In multi-fluid electrospun fibers, each layer/compartment is purposefully designed for specific functionalities. These advancements empirically validate the process–structure–property relationships in electrospun nanomaterials, demonstrating how tailored fabrication strategies translate to enhanced performance in drug delivery, tissue engineering, and beyond. With ongoing technological advancements and the accumulation of emerging needs, it is anticipated that electrospinning will enable the fabrication of more complex multi-chambered nanostructured fibers in the foreseeable future.[113]

2.3. Electrospun nanofiber-based IDDS for BC therapy

Current BC treatment strategies are tailored based on patient-specific factors, tumor type, and metastatic progression, with primary modalities including chemotherapy, radiotherapy, targeted therapy, immunotherapy, and surgical intervention.[5] While chemotherapy and radiotherapy effectively eradicate tumor cells, their inherent high cytotoxicity indiscriminately damages healthy tissues, with certain chemotherapeutic agents inducing severe complications such as hepatotoxicity, nephrotoxicity, and pulmonary toxicity.[114] Additionally, multidrug resistance (MDR) in tumors significantly diminishes therapeutic efficacy.[115] To mitigate these systemic side effects, researchers have pursued targeted therapy, which employs molecularly specific agents to act on oncogenic sites (*e.g.*, *HER2*, EGFR), thereby reducing drug dosage and selectively inducing tumor cell apoptosis with minimized off-target toxicity compared to conventional chemotherapy.[116,117] However, tumor heterogeneity—characterized by diverse genomic subclones within the tumor microenvironment—and the emergence of drug-resistant subpopulations often lead to imprecise diagnostic biopsies and suboptimal clinical outcomes.[116] Immunotherapy, also termed biologic therapy, harnesses the immune system to recognize and eliminate malignant cells through mechanisms such as immune checkpoint inhibitors (*e.g.*, anti-*PD-1*/*PD-L1* antibodies) and CAR-T cell therapy.[118] Although immunotherapy represents a paradigm shift in oncology, challenges persist, including unavoidable immune-related adverse events (irAEs), uncertainties in optimal dosing protocols, and patient-specific variability in therapeutic responses, which complicate its universal clinical adoption.[119,120] Ensuring both safety and efficacy remains a critical challenge for the clinical translation of immunotherapeutic strategies.[121]

For BC, surgical resection remains the most effective therapeutic approach. Despite advancements in surgical techniques, even with clear margins of normal tissue post-resection, locoregional residual cancer cells and disseminated solitary tumor cells during surgery may still lead to tumor recurrence.[122] Consequently, postoperative chemotherapy/radiotherapy is often required. However, conventional chemotherapy induces systemic adverse effects and MDR, resulting in suboptimal therapeutic outcomes.[123] In contrast, IDDS enable localized delivery of optimized drug doses directly to the tumor site, eliminating systemic drug migration through the bloodstream while enhancing targeted therapeutic efficacy.[124] Thus, localized drug delivery strategies are imperative to amplify antitumor effects while minimizing damage to healthy tissues.

As a prominent branch of nanocarriers, electrospun nanofibers exhibit exceptional potential in biomedical applications due to their low cost, high drug-loading capacity, large specific surface area, structural mimicry of native extracellular matrix, and compatibility with multimodal therapies. When implanted at tumor sites, electrospun nanofibers establish localized drug delivery platforms that not only increase drug concentration at the target region and reduce systemic toxicity but also enable precise control over drug release kinetics. Furthermore, the use of biodegradable polymer matrices ensures high biocompatibility, allowing seamless integration with host tissues post-implantation. Consequently, electrospun nanofiber-based IDDS are increasingly recognized as promising candidates for localized postoperative cancer therapy.[125]

This article categorizes recent advances in electrospun nanofiber IDDS for BC treatment into two classes: conventional drug-loaded systems and functional responsive systems. The former is classified by the source of anticancer agents (*e.g.*, synthetic drugs, natural compounds), while the latter is organized based on stimuli-responsive components (*e.g.*, pH-sensitive nanoparticles, photothermal agents).

3. Drug-loaded electrospun nanofiber-based IDDS for BC therapy

3.1. Electrospun nanofiber IDDS loaded with natural drugs

Natural drugs now play a pivotal role in cancer therapy, with a significant proportion of clinically used anticancer agents originating from natural sources such as plants, animals, and microorganisms.[126] Natural compounds exhibit robust anticancer activity, counteracting BC aggressiveness by inhibiting tumor cell proliferation and modulating cancer-associated signaling pathways.[127] Their low toxicity profile further positions them as advantageous candidates for BC treatment. Consequently, recent studies have increasingly integrated natural drugs/extracts into electrospun nanofibers for implantation at tumor sites to evaluate their antineoplastic efficacy against BC cells.

Laetrile (D-mandelonitrile-β-glucuronide), a cyanogenic glycoside derived from amygdalin (AMG), has been utilized as a complementary and alternative natural agent in cancer therapy for over three decades.[128] Seyhan *et al.*[129] employed microwave-assisted extraction[130] to isolate AMG from apricot kernels, subsequently fabricating electrospun PLA/polyethylene glycol (PEG)/AMG nanofibers. Compared to other formulations, nanofibers loaded with 20 mg AMG demonstrated sustained local drug release, exhibiting enhanced cytotoxicity against MCF-7 BC cells while mitigating postoperative recurrence risks, thus enabling direct implantation into solid tumors for targeted therapy.

Natural red pigments, such as prodigiosin (PG), exhibit immunosuppressive properties and pro-apoptotic effects *in vitro*, alongside demonstrated antitumor activity *in vivo*.[131] Akpan *et al.*[132] developed hybrid composite nanofibers by blending PG, poly(D,L-lactide-*co*-glycolide) (PLGA), gelatin (Gel), and Pluronic F127. These fibers not only enhanced cellular adhesion but also improved sustained drug release kinetics, offering a dual-functional platform for localized cancer treatment.

Taxanes, a class of antitumor agents isolated from plants, represent a breakthrough in BC therapy as adjuvant agents, marking the advent of a new era in early-stage BC treatment.[133] To enhance chemotherapy efficacy for triple-negative BC (TNBC) while avoiding systemic toxicity, Hsu *et al.*[134] developed a metronomic chemotherapy strategy utilizing paclitaxel (PTX)-loaded PLGA nanofibers as localized implantable membranes (Fig. 3A(a)). Compared to intravenous PTX injection, subcutaneous implantation of these drug-eluting fibrous membranes achieved sustained drug release and site-specific therapy through direct targeting and tumor microenvironment modulation. This approach not only significantly reduced tumor growth rates (Fig. 3A(b)) but also minimized systemic toxicity, demonstrating superior therapeutic efficacy and safety over conventional chemotherapy.

Polyphenolic compounds, abundantly present in plants, exhibit multifaceted anticancer properties, including inhibition of cancer cell proliferation, suppression of tumor growth and metastasis, and induction of apoptosis.[135] Chen *et al.*[136] engineered a novel alginate/Gel sponge integrated with Cur-loaded electrospun fibers (CFAGS) through a combined strategy of electrospinning and interpenetrating polymer networks (IPNs), designed for rapid hemostasis and prevention of tumor recurrence (Fig. 3B(a and b)). Experimental results demonstrated that CFAGS controlled Cur release, enabling localized Cur accumulation at surgical tumor sites to effectively suppress postoperative local recurrence in a subcutaneous tumor recurrence model (Fig. 3B(c and d)). Furthermore, the sponge exhibited excellent biocompatibility, safely integrating into host tissues without inducing toxicity in normal organs or tissues. This innovative approach represents a pioneering strategy for implanting dual-functional sponges at postoperative sites as adjunctive therapy in cancer surgery.

Alkaloids, recognized as the most bioactive compounds in natural herbs, serve as critical sources for numerous commercially available pharmaceuticals.[137] Piperine (PIP), a phytochemical derived from black pepper, demonstrates multifaceted therapeutic properties including anticancer, antiarthritic, antimicrobial, antioxidant, and anti-inflammatory activities. Jain *et al.*[138] engineered PIP-loaded polycaprolactone (PCL)/Gel blend nanofibers *via* electrospinning, which exhibited sustained drug release profiles. The released PIP suppressed MCF-7 BC cell growth through reactive oxygen species (ROS) generation and G2/M cell cycle arrest, while showing minimal cytotoxicity toward non-cancerous cells (Fig. 4A). These findings highlight the potential of PIP-incorporated nanofiber mats as implantable biodegradable patches for postoperative cancer management. Expanding on this, Babadi *et al.*[139] developed a collagen (Coll)-functionalized PCL-based electrospun nanofiber system loaded with PIP (PIP-PCL75-Coll25) to enhance hydrophilicity. Histopathological analysis revealed significantly elevated caspase-3-positive cells ($P < 0.001$) and reduced Ki-67 expression in tumor sections from mice treated with PIP-PCL75-Coll25 (Fig. 4B), confirming enhanced apoptosis induction and antiproliferative efficacy. Capsaicin (*trans*-8-methyl-*N*-vanillyl-6-nonenamide*), a hydrophobic, crystalline alkaloid and primary pungent component in chili extracts,[140] was incorporated into a novel nanodelivery platform by Ahmady *et al.*[141] Utilizing cationic gemini surfactant-stabilized nanoemulsions, capsaicin-loaded alginate nanoparticles were synthesized and embedded into PCL-chitosan (CS) nanofibers *via* electrospinning. This hybrid system extended capsaicin release from 120 h to over 500 h, effectively inhibiting MCF-7 cell proliferation while maintaining biocompatibility with human dermal fibroblasts (Fig. 4C).

Flavonoids, a subclass of polyphenols ubiquitously found in plants, exhibit nontoxic multifunctional bioactivities such as carcinogen inactivation, apoptosis induction, and MDR reversal.[142] Ganesan *et al.*[143] engineered coaxial electrospun isoorientin-loaded (ISL) nanofiber scaffolds (ISL-NF) through cryo-cutting techniques (Fig. 4D). ISL-NF demonstrated robust suppression of BC growth and metastasis both *in vitro* and *in vivo*, with 24-hour treatment significantly impairing cell proliferation, migration, and apoptosis resistance across multiple BC cell lines.

Terpenoids, predominantly plant-derived compounds, exhibit multifaceted antitumor properties including antiproliferative, pro-apoptotic, antiangiogenic, and antimetastatic activities.[144] Eslami Vaghar *et al.*[145] engineered electrospun PLGA nanofibers embedded with artemisinin (Art)-loaded mesoporous silica nanoparticles (MSNs) (Art@MSNs-PLGA NFs). Experimental findings demonstrated that the pro-apoptotic Art@MSNs-PLGA NFs exhibited enhanced efficacy over free Art in selectively targeting SK-BR-3 BC cell viability and proliferation.

3.2. Electrospun nanofiber-based IDDS loaded with chemotherapeutic agents

Chemotherapeutic agents, synthetic compounds designed to target tumor cell proliferation *via* apoptosis and autophagy pathways, inhibit or eliminate cancer cells by disrupting criti-

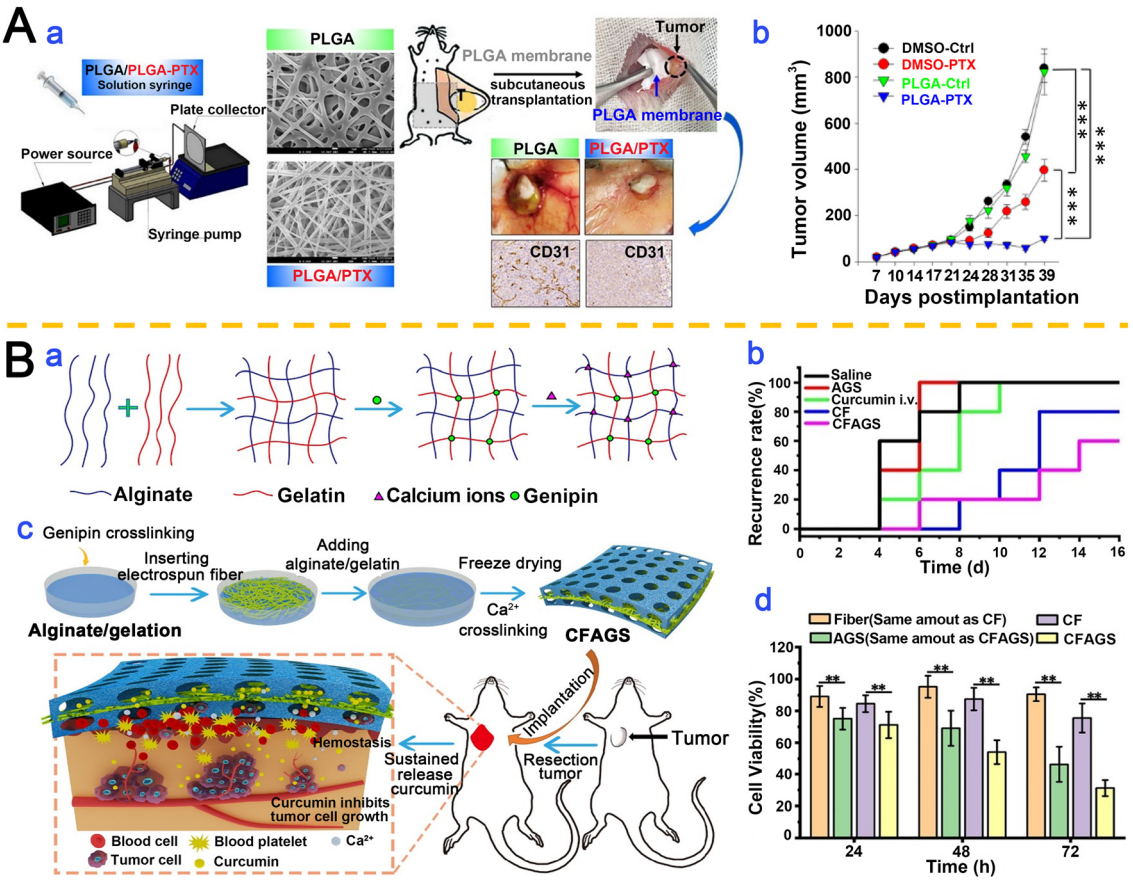

Fig. 3 Application of taxanes (A) and polyphenolic compounds (B) in electrospun nanofiber IDDS. A. Therapeutic efficacy of PTX in TNBC: (a) synergistic tumor suppression *via* metronomic chemotherapy and a PTX-loaded PLGA nanofiber system. (b) Tumor growth kinetics in MDA-MB-231-Luc xenografts treated with the system. Tumor volumes (mean ± SD, n = 5) were calculated and monitored over time. Reproduced from ref. 134 with permission from Multidisciplinary Digital Publishing Institute, copyright 2021.[134] B. Development of a hybrid alginate/gelatin sponge (AGS): (a) fabrication schematic of the genipin/CaCl crosslinked AGS. (b) Design of a curcumin-loaded electrospun fiber-integrated AGS or intraoperative hemostasis and postoperative anti-recurrence. (c) Comparative local tumor recurrence rates. (d) Time-dependent cytotoxicity of various formulations against MCF-7 cells. Reproduced from ref. 136 with permission from Elsevier, copyright 2021.[136]

cal growth cycles, including inducing cell cycle arrest.[146] Despite their efficacy in oncology, systemic administration of these agents often leads to severe side effects and long-term sequelae, necessitating localized delivery strategies.[147] Electrospun nanofiber-based IDDS have emerged as a transformative approach for site-specific anticancer drug delivery, minimizing systemic toxicity while maximizing therapeutic precision.[148,149]

Anticancer antibiotics, particularly DNA-intercalating agents and repair inhibitors, represent a pivotal class of chemotherapeutics.[150] Yang *et al.*[151] pioneered a hybrid system integrating actively targeted micellar systems with implantable core–shell nanofibers. Folate (FA)-conjugated PCL-PEG copolymers self-assembled into targeted micelles encapsulating DOX, which were subsequently embedded into nanofibers. Sustained micelle release *via* fiber degradation enabled tumor-selective accumulation through enhanced permeability and retention (EPR) effects and FA receptor-mediated endocytosis (Fig. 5A). Li *et al.*[152] engineered a hierarchical ultrafiber device co-loaded with DOX hydrochloride (DOX·HCl) and the MMP-2 inhibitor disulfiram (DSF) for postoperative BC therapy (Fig. 5B). This system achieved rapid DOX·HCl release to eliminate residual tumor cells, coupled with sustained DSF delivery to suppress metastasis. In a separate study, Li *et al.*[153] developed biodegradable PLGA nanofiber membranes (DOX-MPs/ASA@NF) for co-delivery of DOX-loaded tumor-repopulating cell-derived microparticles (DOX-MPs) and aspirin (ASA). The platform enabled time-programmed release: DOX-MPs eradicated residual cancer cells, while ASA inhibited platelet-driven tumor proliferation and metastasis, significantly reducing postoperative recurrence. Further advancing spatiotemporal control, Li *et al.*[154] utilized microfluidics-inspired triaxial electrospinning to fabricate triple-layered fibrous devices with hollow lumens. Hydrophilic DOX was encapsulated within the lumen for rapid release (modulated by wall thickness), while hydrophobic apatinib (Apa), a tumor angiogenesis inhibitor, was embedded in the fiber matrix for sustained release. Subcutaneous implantation in murine models demonstrated

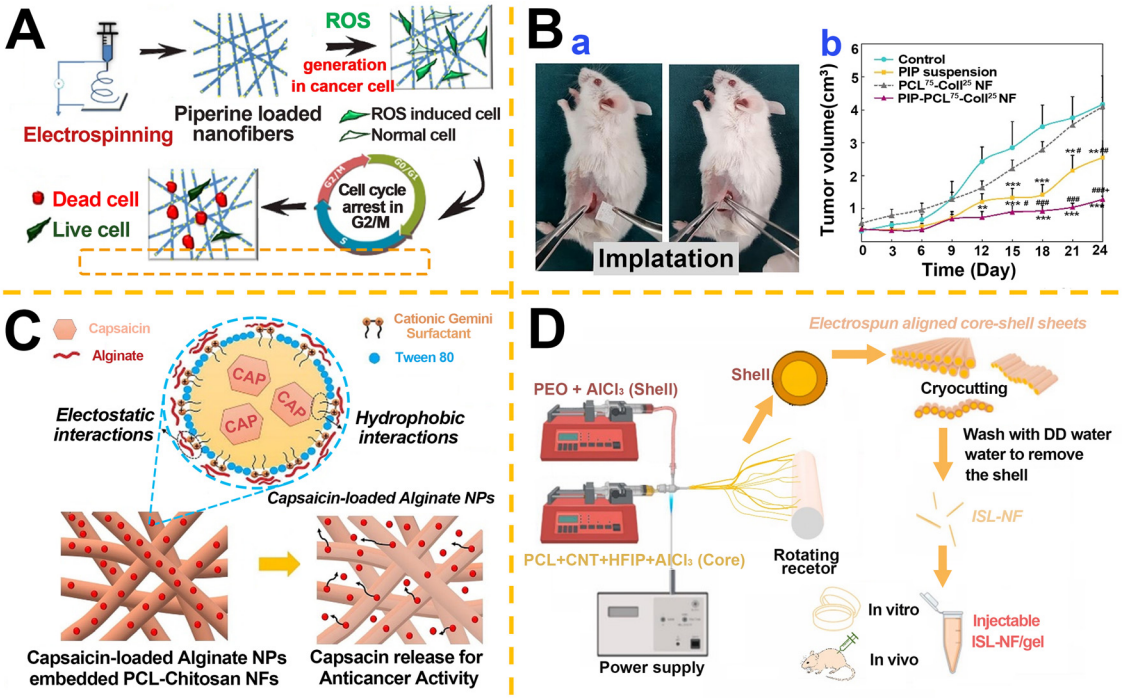

Fig. 4 Application of alkaloid (A–C) and flavonoid (D) compounds in electrospun nanofiber IDDS. A. PIP-loaded PCL/Gel nanofibers induced cancer cell apoptosis *via* sustained PIP release, ROS generation, and G2/M-phase arrest. Reproduced from ref. 138 with permission from American Chemical Society, copyright 2016.[138] B. *In vivo* therapeutic evaluation: (a) surgical implantation of nanofiber systems. (b) Tumor growth kinetics showing superior suppression by PIP-loaded nanofibers *versus* controls (PIP suspension, blank fibers). Data: mean volume ± SEM (n = 5–7 per group). Reproduced from ref. 139 with permission from Elsevier, copyright 2022.[139] C. Fabrication of Cap-ALG NPs@PCL-CS hybrid nanofibers *via* emulsion-electrospinning, using a gemini surfactant to encapsulate capsaicin. Reproduced from ref. 141 with permission from Elsevier, copyright 2023.[141] D. Production of ISL-loaded nanofibers (ISL-NFs) by coaxial electrospinning, cryo-cutting, and selective shell dissolution. Reproduced from ref. 143 with permission from Elsevier, copyright 2024.[143]

synergistic therapeutic efficacy through temporally staggered drug release, establishing this platform as a versatile tool for localized, time-programmed multidrug delivery in oncology.

Metal-based anticancer agents exhibit broad therapeutic potential in oncology due to their ability to induce intracellular ROS generation, oxidative stress, and apoptotic cell death through diverse molecular mechanisms.[155,156] For instance, gold nanoparticles (AuNPs) interact with the acidic tumor microenvironment to amplify oxidative stress *via* ROS production, triggering cancer cell damage and apoptosis. Similarly, silver nanoparticles (AgNPs) demonstrate antiproliferative, pro-apoptotic, and antiangiogenic effects against malignant cells.[157] Arumugam *et al.*[158] fabricated silk fibroin (SF)/cellulose acetate (CA)/Au–Ag nanoparticle composite nanofibers *via* electrospinning for anticancer applications (Fig. 5C). SF and CA acted as dual reductants and stabilizers for Ag and Au ions, synergistically enhancing cytotoxicity against MCF-7 and MDA-MB-231 BC cells (IC_{50} = 17.54 μg mL^{-1}). The crystalline domains within SF enable controlled drug release and preservation of therapeutic bioactivity.[159] Drugs bound to SF are released only upon degradation of the SF-polymer matrix, optimizing therapeutic efficacy. Leveraging this property, Laiva *et al.*[160] developed PCL/SF composite nanofiber scaffolds loaded with titanocene dichloride, achieving controlled drug release to induce apoptosis in MCF-7 cells while serving as a structural support for cell growth (Fig. 5D).

Antimetabolites, analogs of natural metabolites that disrupt DNA/RNA synthesis, are widely employed in cancer therapy due to their selective inhibition of rapidly proliferating malignant cells.[161] Jaisankar *et al.*[162] engineered a methylcellulose (MC)/PLA/PEG hybrid nanofiber mat loaded with 5-FU and Fe_3O_4 nanoparticles. This system demonstrated enhanced anticancer activity (78% inhibition) against MDA-MB-231 cells, with 15.86% of 5-FU synergizing with Fe_3O_4-generated radicals ($O_2^{\bullet-}$, H_2O_2, $OH^{\bullet}$) *via* Fenton reactions to eradicate tumors within 24 hours (Fig. 5E). In immunotherapy, Kuang *et al.*[163] designed an implantable sponge-nanofiber Janus scaffold integrating lyophilized inactivated tumor cells, imiquimod (an immunoadjuvant), and spatially segregated 5-FU. The sponge compartment functioned as an immune niche to activate antitumor responses, while 5-FU-loaded nanofibers mechanically reinforced the scaffold and remodeled the immunosuppressive tumor microenvironment by depleting myeloid-derived suppressor cells (MDSC) (Fig. 5F).

Hormonal therapies, such as tamoxifen citrate (TMX), exert anticancer effects by binding to estrogen receptors to inhibit BC-associated gene expression, suppressing proliferation, inducing apoptosis, and reducing cholesterol synthesis.[164–166]

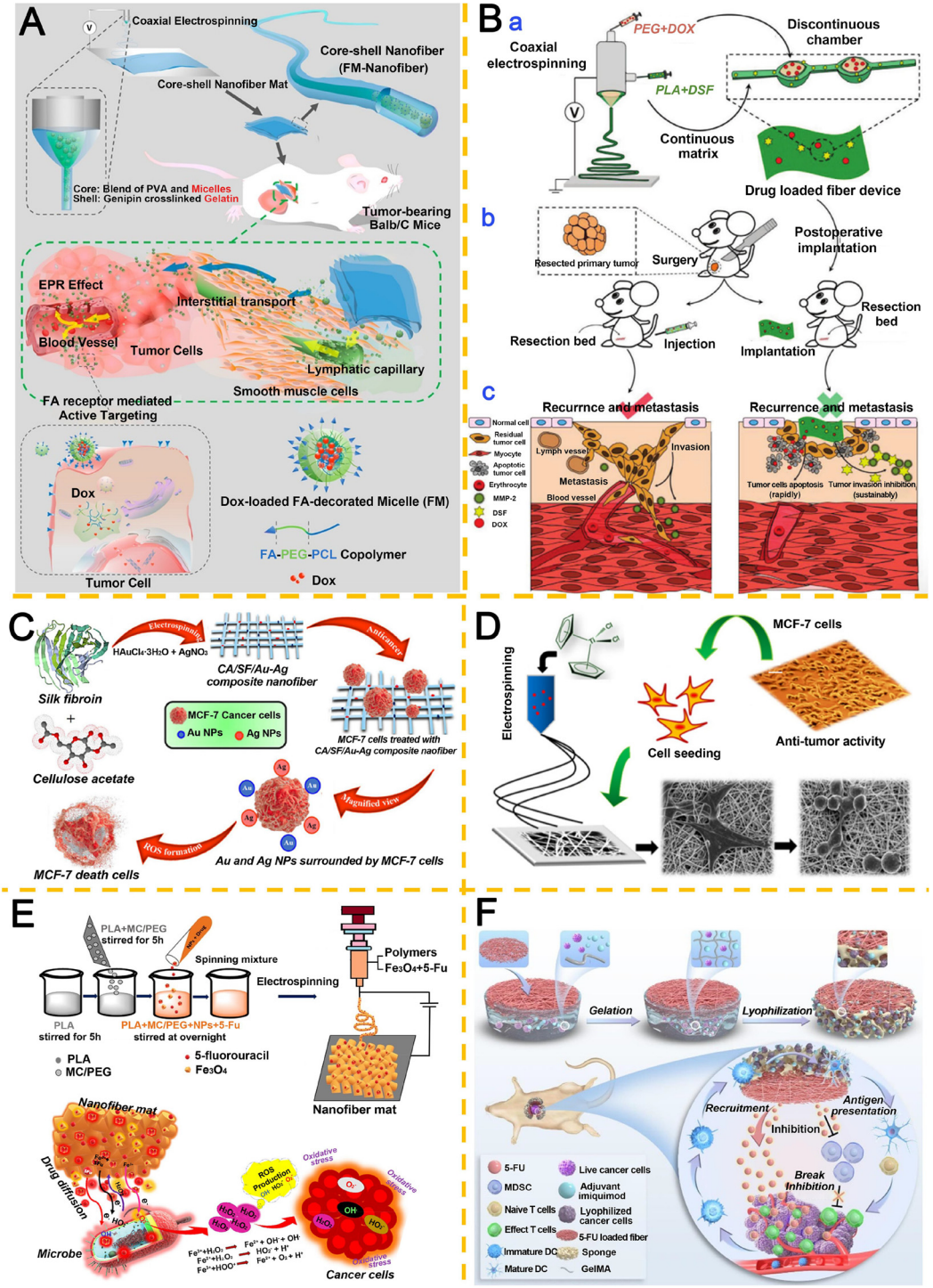

Fig. 5 Application of anticancer antibiotics (A, B), metal-based agents (C, D), and antimetabolites (E, F) in electrospun nanofiber IDDS. A. Active-targeting micelle-nanofiber hybrid (FM-nanofiber): (a) fabrication of FA-conjugated micelles in nanofibers. (b) Tumor-targeting *via* EPR effect and FR-mediated endocytosis. Reproduced from ref. 151 with permission from American Chemical Society, copyright 2015.[151] B. Hierarchical coaxial fiber for post-op therapy: (a) fabrication of DSF/DOX·HCl core–shell fibers. (b) Local *vs.* systemic treatment. (c) Dual-drug release for anti-recurrence (DOX) and anti-metastasis (DSF). Reproduced from ref. 152 with permission from Wiley, copyright 2020.[152] C. Cellulose CA/SF/Au–Ag nanofibers: SF and cellulose CA reduce/stabilize Ag/Au ions, yielding biocompatible fibers with high cytotoxicity to MCF-7 cells (IC_{50} = 17.54 μg mL^{-1}). Reproduced from ref. 158 with permission from Elsevier, copyright 2021.[158] D. PCL/SF nanofiber scaffolds for sustained release of titanocene dichloride to regulate MCF-7 cell proliferation. Reproduced from ref. 160 with permission from Elsevier, copyright 2015.[160] E. 5-FU/Fe_3O_4 nanofiber mats induce rapid tumor cell death (78% inhibition in 24 h) *via* synergistic 5-FU diffusion and Fe_3O_4-mediated Fenton reaction. Reproduced from ref. 162 with permission from American Chemical Society, copyright 2024.[162] F. Janus scaffold for chemoimmunotherapy: integrates a lyophilized sponge (inactivated tumor cells/imiquimod) to initiate immunity and 5-FU-nanofibers to kill residual cells/suppress MDSCs. Reproduced from ref. 163 with permission from Elsevier, copyright 2023.[163]

Pinzón-García *et al.*[167] developed TMX-loaded PCL nanofibers capable of sustained drug release over 14 hours, offering localized TMX delivery to minimize off-target effects on endometrial and hepatic tissues while maintaining therapeutic efficacy.

3.3. Electrospun nanofiber IDDS co-loaded with natural and chemotherapeutic agents

Despite their cornerstone status in BC management, the clinical utility of chemotherapeutic drugs is severely hampered by dose-limiting systemic toxicities and the inevitable emergence of chemoresistance. To address these limitations, research and clinical efforts have shifted toward combining conventional chemotherapy with natural products to amplify therapeutic outcomes through synergistic antitumor effects. Incorporating natural compounds into chemotherapeutic regimens aims to broaden the therapeutic window of cytotoxic drugs while mitigating resistance development.[168]

Co-delivery of chemotherapeutics and plant-derived natural agents *via* nanoscale DDS not only enhances cytotoxicity against cancer cells but also reduces off-target toxicity in healthy tissues. Li *et al.*[169] resolved the challenges of combinatorial delivery of quercetin (Que) and TMX by developing triple-compartment composite nanofibers *via* a tri-fluid electrospinning process (Fig. 6A(a and b)). This innovative design, integrating core–shell and Janus architectures, improved oral bioavailability and potentiated their synergistic activity against BC (Fig. 6A(c)). Chen *et al.*[170] applied localized therapy using electrospun dual-drug (DOX and PTX) fiber membranes. The system achieved sequential drug release: rapid DOX release for immediate tumor cell eradication, followed by sustained PTX release to maintain therapeutic concentrations in an orthotopic mammary model, effectively mini-

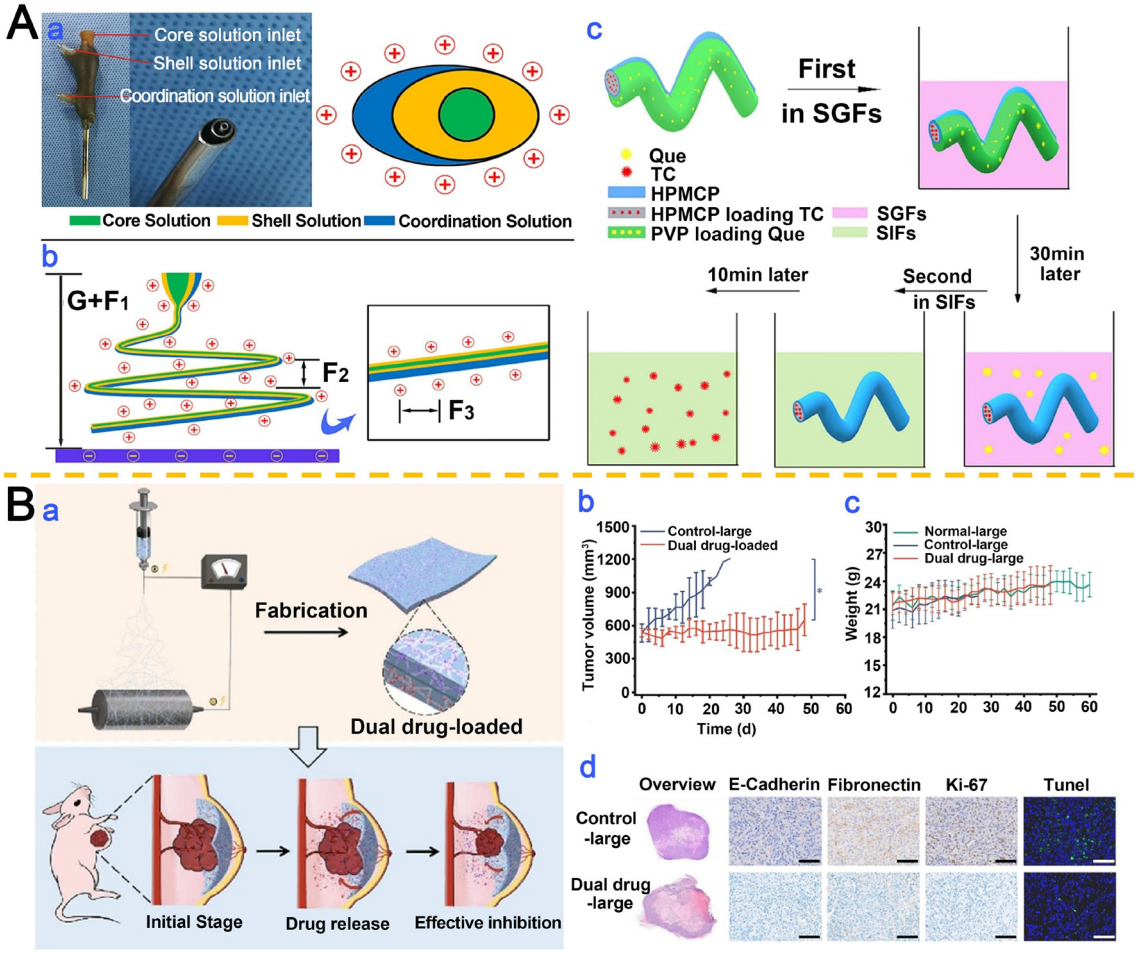

Fig. 6 Research on the dual-loading of natural medicines and chemotherapeutic drugs in electrospun nanofiber-based IDDS. A. Tri-fluid electrospinning for tri-chamber nanofibers: (a) spinneret configuration with three distinct fluids. (b) Compound Taylor cone evolution under multifactorial forces (G, F_1, F_2, F_3). (c) Sequential release profiles of Que and a therapeutic compound. Reproduced from ref. 169 with permission from Elsevier, copyright 2024.[169] B. Antitumor efficacy of drug-eluting membranes: (a) fabrication and hypothesized mechanism of localized tumor suppression. (b) Significant tumor growth inhibition in a large-tumor model. (c) Body weight trends indicating systemic tolerance. (d) Histopathological (H&E, E-cad/fibronectin) and immunohistochemical (Ki67, TUNEL) analyses confirming suppressed tumor viability. Reproduced from ref. 170 with permission from Elsevier, copyright 2023.[170]

mizing local tissue toxicity even at low doses (Fig. 6B). Famta *et al.*[171] engineered nanofibers co-loaded with resveratrol (RES) and DOX as post-surgical implants. *In vitro* evaluations revealed synergistic activity against metastatic MDA-MB-231 cells, with cell cycle analyses showing G2/M phase arrest by DOX and G0/G1 phase arrest by RES. Sustained drug release from the nanofibers reduced DOX-induced necrotic cell death while promoting apoptosis *via* co-delivery, highlighting a promising strategy for adjuvant therapy.

Multilayered DDS enable precise modulation of drug dosage and release kinetics for combination therapies. Najjari *et al.*[172] engineered both monolayer and trilayer electrospun PCL/Gel nanofibers loaded with PTX and 5-FU. The trilayer system (PCL/Gel-PCL/PTX/Gel/5-FU-PCL/Gel) demonstrated superior drug-loading efficiencies of 97% (PTX) and 98% (5-FU), compared to 85% and 87% in monolayer counterparts (PCL/PTX and Gel/5-FU). This hierarchical architecture significantly enhanced therapeutic efficacy against MCF-7 BC cells, attributed to optimized drug retention and controlled elution.

The tumor stroma plays a pivotal role in solid tumor progression, metastasis, and chemoresistance, with cancer-associated fibroblasts driving stromal remodeling and fostering therapeutic resistance through bidirectional crosstalk. Mostafa *et al.*[173] developed PAK1 inhibitor (FRAX597)- and PTX-co-loaded electrospun matrices to disrupt stromal–tumor interactions. Dual-drug fibers suppressed heterospheroid growth and viability by >90%, outperforming single-drug systems. This work introduced a novel therapeutic paradigm leveraging PAK1 inhibition to potentiate localized chemotherapy *via* nanofiber-mediated delivery, particularly for unresectable or residual tumors. Alabrahim *et al.*[174] harnessed the anticancer and anti-inflammatory properties of Pistacia lentiscus essential oil (PLEO), co-electrospinning it with 5-FU into PCL nanofibers. The composite fibers exhibited enhanced thermal stability, mechanical integrity, and tensile strength. PLEO-loaded fibers demonstrated potent antioxidant activity and superior anticancer effects compared to free compounds, underscoring the synergistic benefits of natural extract–polymer hybrid systems.

Recent advances in electrospun IDDS for BC, including diverse drug combinations and functional designs, are comprehensively summarized in Table 3.

4. Stimuli-responsive electrospun nanofiber IDDS for BC therapy

Stimuli-responsive electrospun nanofiber IDDS enhance therapeutic precision by improving the solubility and stability of

Table 3 Recent advances in electrospun nanofiber-based IDDS for BC

Classification	Drug	Polymer	Formulation	Structure	Therapy	Ref.
Taxanes	PTX	PCL/CS	PCL/CS/PTX	Core–shell	Chemotherapy	175
Taxanes	PTX	Poly(glycolide-ε-caprolactone) (PGCL)/PLGA	PGCL/PLGA/PTX	—	Chemotherapy	176
Polyphenols	CUR	PLGA	PLGA/CUR	—	Chemotherapy	177
Polyphenols	CUR	PCL/PEO	PCL/PEO/CUR	—	Chemotherapy	178
Polyphenols	CUR/chrysin (Chr)	PLGA/PEG	PLGA/PEG/CUR/Chr	—	Chemotherapy/dual drugs	179
Polyphenols	RES/xanthohumol (XAN)	PLGA	PLGA/RES/XAN	Core–shell	Chemotherapy/dual drugs	180
Polyphenols	FA	PLGA/PEO	PLGA/PEO/FA	—	Chemotherapy	181
Alkaloid	Hydroxycamptothecin (HCPT)	Poly(DL-lactic acid)–poly(ethylene glycol) (PELA)	PELA/HCPT	—	Chemotherapy	182
Flavonoid	Que	PLA/PEO	PLA/PEO/Que	—	Chemotherapy	183
Antibiotic	DOX	PCL/poly(amido-amine) (PAMAM)	PAMAM/DOX	—	Chemotherapy	184
Antibiotic	DOX	PCL/PEO	PCL/PEO/DOX	Core–sheath	Chemotherapy	185
Antibiotic	DOX·HCl	PCL	PCL/DOX·HCl	—	Chemotherapy	186
Antibiotic	DSF	CA/PEO	CA/PEO/DSF	—	Chemotherapy	187
Metals	Cisplatin	CS/*N*-vinylcaprolactam (NVCL)	CS-g-PNVCL/Cis	—	Chemotherapy	188
Metals	AgNP/niclosamide	PEO/PCL	PEO/Nic@AgNP	—	Chemotherapy/dual drugs	189
Metals	Tecoflex™ EMs-BisBAL NPs	Polyurethane (PU)	PU@ BisBAL NPs	—	Chemotherapy	190
Antimetabolites	5-FU	PCL	PCL/5-FU	—	Chemotherapy	191
Antimetabolites	5-FU	PCL/MC/PEG	PCL/MC/PEG/5-FU	—	Chemotherapy	192
Multi-drug	Camel alkaloids/nidaplatin	PCL	N + L@PCL	—	Chemotherapy/dual-drugs	184 and 193
Multi-drug	Berberine (BBR)/DOX	PCL	PCL/BBR/DOX	—	Chemotherapy/dual-drugs	194
Multi-drug	TMU340/DTX	PVA	PVA/TMU340/DTX	—	Chemotherapy/dual-drugs	195
Multi-/dual	CUR/CS derivatives	PVA	PVA/CUR/CS-DS	—	Chemotherapy/dual-drugs	196

hydrophobic drugs, augmenting localized drug payloads, and prolonging systemic circulation durations.[197] Despite their pharmacokinetic advantages, conventional passive targeting strategies relying on the EPR effect often suffer from limited tumor penetration and dose-dependent off-target toxicity.[198] To address these limitations, microenvironment-responsive IDDS leverage tumor-specific stimuli—such as pH gradients, enzymatic activity, or external triggers (light, magnetic/electric fields)—to achieve spatiotemporally controlled "on-demand" drug release,[199] minimizing collateral tissue damage while maximizing therapeutic efficacy.[57,200–202]

Central to these systems are biocompatible smart materials —such as photosensitizers, photothermal agents, magnetic nanoparticles, and stimulus-sensitive polymers—which undergo specific physicochemical changes including protonation, chemical bond cleavage, structural rearrangement, or energy transfer in response to internal or external triggers.[56,57] Endogenous stimuli primarily originate from the tumor microenvironment, including pH variations, redox gradients, and specific enzymes,[203–205] while exogenous stimuli involve externally applied light, magnetic fields, or electric fields.[206–208] A summary of the advantages and limitations of different SRDDS is provided in Table 4.

4.1. Endogenous stimulus-responsive IDDS

In contrast to externally controlled systems, endogenous stimulus-responsive IDDS exploit the inherent pathological abnormalities of the tumor microenvironment. The pH sensitivity of IDDS refers to their ability to undergo rapid structural or functional alterations in response to subtle pH variations within acidic or alkaline microenvironments.[209] Exploiting the physiological pH discrepancy between normal tissues (7.2–7.4) and the acidic extracellular compartments of tumors (6.0–7.0),[210] these systems enable precise spatiotemporal control of drug release at pathological sites. Organic nanoparticles, inorganic nanoparticles, and hybrid organic–inorganic nanoparticles have been extensively explored as pH-responsive nano-IDDS for such applications.

Mehnath *et al.*[211] engineered pH-responsive core–shell nanofibers *via* coaxial electrospinning of PTX-loaded CA-conjugated poly(bis(carboxyphenoxy)phosphazene) (PCPP) polymeric micelles. The stimuli-responsive nanofibers exhibited exceptional H^+ absorption and cation exclusion properties, achieving maximal swelling to enhance drug release under acidic conditions. Sustained PTX release over 180 hours at target sites significantly reduced systemic toxicity while suppressing MCF-7 BC cell proliferation through ROS generation and cell cycle arrest (Fig. 7A).

To mitigate chemotherapy-induced cytotoxicity and MDR, Zhu *et al.*[212] developed an electrospun nanofiber scaffold for co-delivery of DOX and small interfering RNA (siRNA). DOX was first intercalated into nanolamellar HAP, which was subsequently incorporated into electrospun PLGA nanofibers. The DOX-loaded LHAP/PLGA scaffold was coated with polydopamine (PDA) and functionalized with siRNA/polyethyleneimine (PEI) complexes. Owing to its pH-dependent degradability, the scaffold demonstrated synchronized release of DOX and siRNA in acidic tumor microenvironments (Fig. 7B). The synergistic effect of DOX and siRNA resulted in superior therapeutic efficacy *in vitro* and *in vivo* compared to single-drug-loaded scaffolds, with no detectable toxicity or adverse effects in murine models.

Rakhshani *et al.*[213] developed a pH-responsive SF membrane co-loaded with DOX-encapsulated PLGA nanoparticles and simvastatin (SV/DOX PLGA/SF) (Fig. 7C), serving as an implantable, biocompatible, and biodegradable platform for postoperative combinatorial BC therapy. The DOX-loaded PLGA nanoparticles were synthesized using a microfluidic reactor (Fig. 7C(a)). Experimental data revealed that SF films crosslinked for 7.5 minutes exhibited a degradation rate of 35.3 ± 2.1% over 21 days. pH-Dependent DOX release from the SV/DOX PLGA/SF system demonstrated cumulative releases of 74.23% at pH 5.5 and 58.91% at pH 7.4 by day 11 (Fig. 7C(b)). MTT assays confirmed the synergistic cytotoxicity of SV and DOX, particularly at concentrations of 35 μM SV and 4 μM DOX after 24 h (Fig. 7C(c)). *In vivo* studies demonstrated that SV/DOX PLGA/SF significantly suppressed tumor recurrence (0.52 ± 0.103% recurrence rate), outperforming DOX PLGA/SF alone. This localized therapeutic approach reduced systemic side effects compared to conventional chemotherapy.

Ductal carcinoma *in situ* (DCIS), characterized by abnormal cell proliferation within breast milk ducts, accounts for 20% of diagnosed BC cases in women. Khatami *et al.*[214] engineered core–shell nanofibers *via* emulsion electrospinning, featuring a Gel core and PLA shell (Fig. 7D(a)). Loading these tubular

Table 4 Release kinetic characteristics and limitations of various SRDDS

Stimulation type	Release kinetic characteristics	Known major drawbacks
pH-Responsive (endogenous)	• Acidic triggering in TME/organelles • Sustained release at physiological pH • Diffusion-dependent	• Limited targeting specificity • Release dependent on material degradation
Light-responsive (exogenous)	• High spatiotemporal precision • Potential for synergistic therapy • Poor tissue penetration	• Limited tissue penetration • Phototoxicity concerns
Magnetic field-responsive (exogenous)	• Remote control with deep penetration • Magnetothermal effects • Complex release mechanism	• Complex and expensive equipment • Potential long-term toxicity
Multi-fluid electrospinning (exogenous)	• Precise controllability • Rapid response • Dependent on conductive materials • Quantitative release capability	• Requires electrode implantation • Uneven field distribution

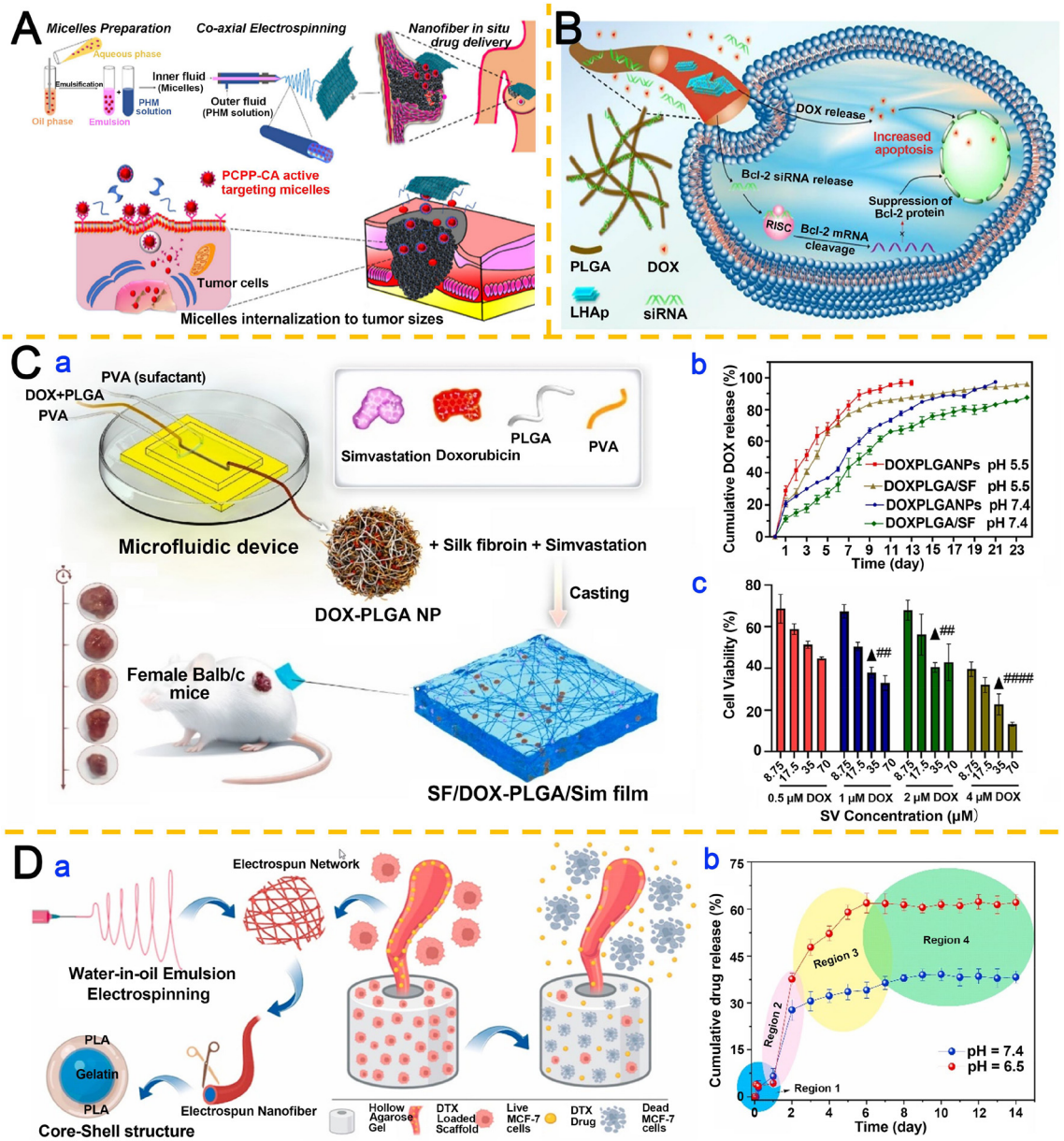

Fig. 7 Research on pH-responsive electrospun nanofiber-based IDDS. A. Coaxial electrospinning of core–shell nanofibers encapsulating PTX-loaded PCPP-CA micelles for pH-responsive and actively targeted drug delivery to breast tumor cells. Reproduced from ref. 211 with permission from Elsevier, copyright 2020.[211] B. pH-Dependent release kinetics of the DOX/HPPP/siRNA scaffold, enabling synchronized DOX and siRNA delivery in acidic tumor microenvironments. Reproduced from ref. 212 with permission from Elsevier, copyright 2023.[212] C. (a) Microfluidic synthesis of DOX-PLGA NPs integrated into SV-functionalized SF membranes for post-op therapy. (b) Enhanced and sustained DOX release from PLGA/SF composites at pH 5.5 (74.23% *vs.* 58.91% by day 11). (c) Synergistic cytotoxicity of DOX and SV against MCF-7 cells. Reproduced from ref. 213 with permission from Elsevier, copyright 2025.[213] D. (a) Emulsion electrospinning of DTX-loaded Gel/PLA core–shell nanofibers for localized MCF-7 cell eradication. (b) Accelerated, pH-responsive DTX release from 3D tubular scaffolds at pH 6.5. Reproduced from ref. 214 with permission from Elsevier, copyright 2023.[214]

scaffolds with the anticancer agent docetaxel (DTX) revealed pH-dependent drug release kinetics, with significantly accelerated elution at pH 6.5 compared to physiological conditions (pH 7.4) (Fig. 7D(b)). This pH-responsive behavior positions the system as a promising platform for enhanced drug delivery to acidic tumor microenvironments. *In vitro* studies demonstrated that DTX-loaded scaffolds achieved potent eradication of MCF-7 BC cells, outperforming non-loaded counterparts, thereby validating their potential for localized chemotherapy with minimized systemic toxicity.

4.2. Exogenous stimulus-responsive IDDS

4.2.1. Light-responsive IDDS. Light stimulation offers spatiotemporally controllable modulation of IDDS through

adjustable power density, irradiation duration, and precise targeting, making it a preferred strategy for on-demand drug release.[215] Light-responsive IDDS enable precise temporal and spatial control of therapeutic payloads, minimizing off-target bioactivity and systemic side effects.[216] These systems typically respond to specific wavelengths (*e.g.* near infrared, NIR), where photothermal transducers generate localized hyperthermia under NIR exposure. The resultant temperature elevation not only induces cancer cell ablation but also enhances tumor vascular permeability, synergizing chemotherapy with phototherapy for improved therapeutic outcomes.[217–219]

Gold nanorods (AuNRs) have emerged as promising photothermal agents due to their biocompatibility, facile synthesis, and strong localized surface plasmon resonance effects.[220,221] Jaswal *et al.*[222] engineered hybrid plasmonic-aligned nanofiber scaffolds by electrospinning AuNRs coated with reduced graphene oxide (rGO, 209 nm) nanosheets and PCL (Fig. 8A). Under 808 nm NIR irradiation (0.72 W cm^{-2}), the AuNR–rGO@PCL nanofibers (optical density 4.0) achieved over 90% eradication of MCF-7 cancer cells while supporting mammary neural tissue regeneration.

Hydrogel-based localized DDS represents a promising approach for treating superficial malignancies. Wei *et al.*[223] developed coaxial electrospun core–shell hydrogel fiber scaffolds featuring a PDA-alginate (15.3 wt%) shell and a drug-loaded thermosensitive hydrogel core (Fig. 8B). NIR-triggered photothermal conversion by PDA elevated fiber temperature, inducing a gel–sol transition in the thermos-responsive core to release encapsulated therapeutics. This system demonstrated synergistic tumor cell elimination and prevention of postoperative recurrence, highlighting its potential as a BC cavity filler post-resection.

DCIS, a non-invasive breast malignancy characterized by malignant epithelial cell accumulation in mammary ducts, may progress to invasive carcinoma if untreated. Sadeghi *et al.*[224] engineered a tri-layered tubular 3D scaffold mimicking the complex DCIS microenvironment for *in vitro* cancer cell culture and combinatorial chemo-photothermal therapy (CPT) (Fig. 8C). Concurrent administration of DTX and laser irradiation on scaffold-cultured MDA-MB-231 cells demonstrated synergistic tumor suppression, achieving 73% cancer cell eradication through combined cytotoxic and photothermal effects.

Cancer stem cells (CSCs), pivotal in tumor initiation and chemoresistance, represent critical therapeutic targets for BC recurrence prevention. Chen *et al.*[225] developed electrospun PCL nanofibers co-loaded with hydroxylated multi-walled

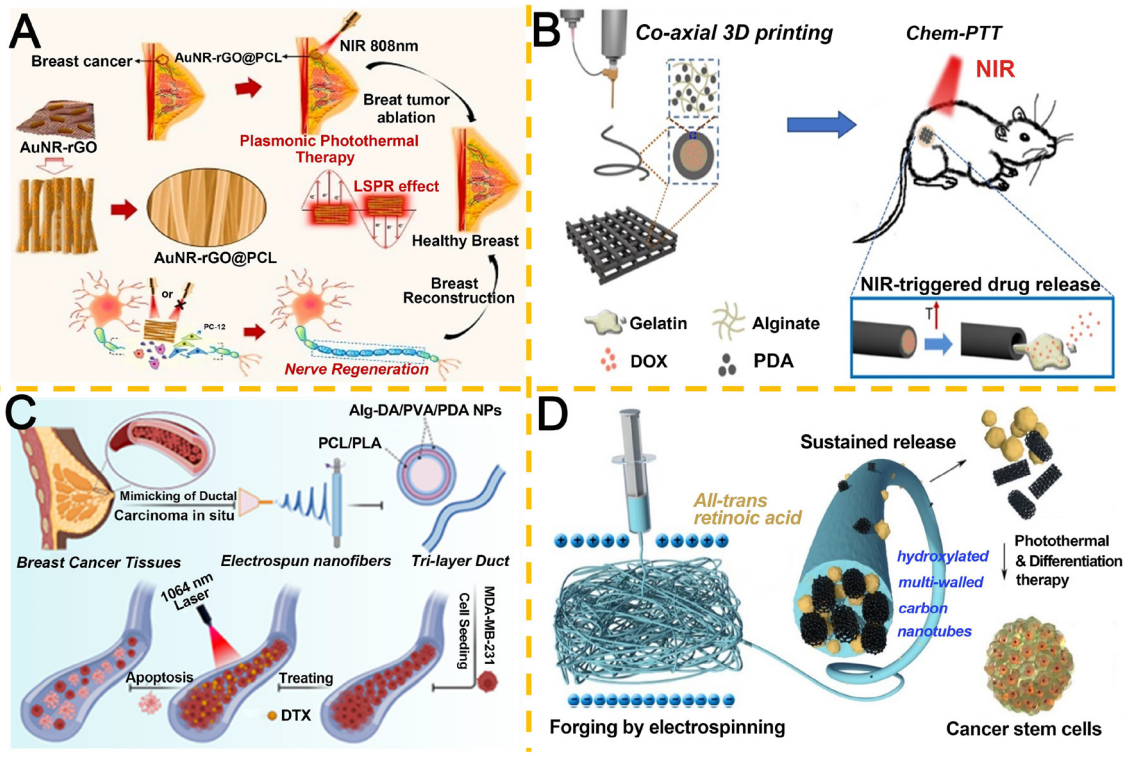

Fig. 8 Research on light-responsive electrospun nanofiber-based IDDS. A. Plasmonic AuNR–rGO@PCL nanofibrous scaffolds for NIR-activated photothermal ablation and neural regeneration. Reproduced from ref. 222 with permission from Elsevier, copyright 2022.[222] B. Coaxial 3D bioprinting of core–shell scaffolds with NIR-triggered sol–gel transitions for controlled drug release. Reproduced from ref. 223 with permission from Elsevier, copyright 2020.[223] C. Biomimetic tri-layered 3D tubular platform to evaluate chemo-photothermal therapy in DCIS-mimetic microenvironments. Reproduced from ref. 224 with permission from American Chemical Society, copyright 2023.[224] D. PCL nanofibers functionalized with MWCNT-OH and ATRA for dual-modal eradication of chemotherapy-resistant CSCs. Reproduced from ref. 225 with permission from Elsevier, copyright 2020.[225]

carbon nanotubes (MWCNTs-OH) as photothermal agents and all-trans retinoic acid (ATRA) for CSC modulation (Fig. 8D). Under NIR irradiation, MWCNTs-OH-generated hyperthermia selectively ablated CSCs, while ATRA induced CSC differentiation into chemotherapy-sensitive phenotypes. This dual-action system combining thermotherapy and differentiation therapy exhibited potent CSC suppression, demonstrating potential as post-surgical implants to prevent BC recurrence.

4.2.2. Magnetic-responsive IDDS. Magnetic Nanoparticles (MNPs) are widely recognized for their ability to generate localized hyperthermia under external magnetic fields, a phenomenon extensively utilized in magnetothermal cancer therapy to enhance drug efficacy.[226–228] The advantages of magnetic-responsive drug delivery lie in the versatility of magnetic field modulation—encompassing static field-guided targeting, alternating magnetic field (AMF)-induced heating, or hybrid modes—while minimizing thermal damage to healthy tissues through controlled MNP-mediated energy conversion.[57,229] Effective magnetic drug carriers require optimized magnetization, biocompatibility, and precise drug loading/release kinetics.[230]

Surface modification of polymers *via* PDA coating offers a facile strategy to enhance interfacial interactions with metal oxides, enabling efficient MNP integration.[231] Materials capable of repeated heat generation under AMF exposure are particularly promising for synergistic thermochemotherapy applications.

To address chemoresistance in BC, Chen *et al.*[232] engineered a PCL-based IDDS co-loaded with MNPs, DOX, and the chemosensitizer Cur (Fig. 9A). This system achieved concurrent release of dual therapeutics with distinct physicochemical properties. MNPs generated hyperthermia under AMF, reversing MDR by enhancing cellular sensitivity to both heat and DOX/CUR. Sustained drug release over two months provided prolonged antitumor efficacy, demonstrating the potential of localized magnetothermal IDDS to improve post-operative outcomes with reduced systemic chemotherapy burden.

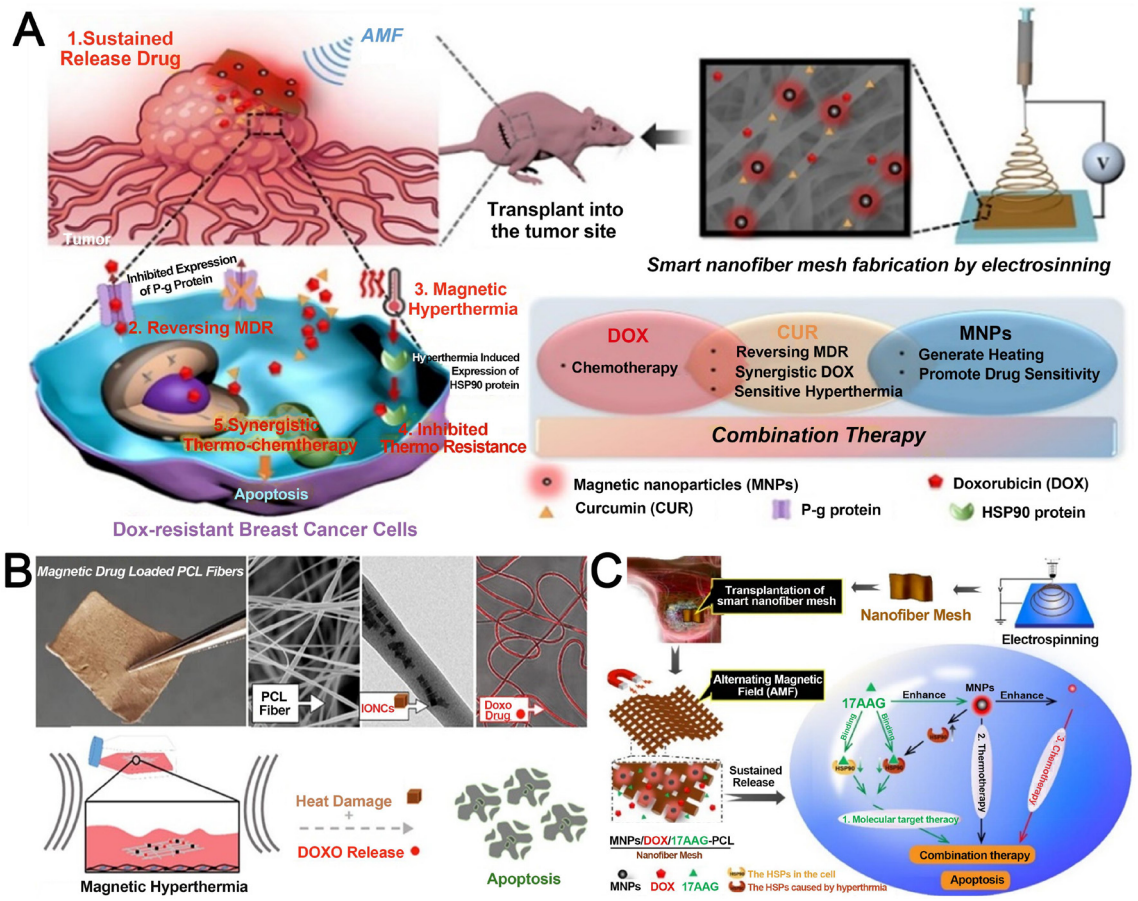

Fig. 9 Research on magnetic-field-responsive electrospun nanofiber-based IDDS. A. Multifunctional nanofiber mesh for the combinatorial suppression of drug-resistant BC *via* co-delivery of MNPs, DOX, and Cur, enabling synchronized magnetothermal–chemotherapy. Reproduced from ref. 232 with permission from Elsevier, copyright 2023.[232] B. Magnetothermal fibers with chain-aligned IONCs and DOX in a PCL matrix, using AMF-triggered hyperthermia to enhance drug penetration and tumor ablation. Reproduced from ref. 233 with permission from Elsevier, copyright 2022.[233] C. Triple-modal therapeutic nanofiber mesh integrating MNPs, DOX, and 17AAG. AMF-induced hyperthermia ablates cells and enhances DOX efficacy, while 17AAG suppresses HSP-mediated thermotolerance. Reproduced from ref. 234 with permission from Multidisciplinary Digital Publishing Institute, copyright 2021.[234]

In a separate approach, Serio *et al.*[233] fabricated MNP/DOX-loaded PCL nanofibers featuring chain-aligned iron oxide nanocubes (IONCs) (Fig. 9B). While these fibers exhibited potent cytotoxicity against DOX-sensitive cervical cancer cells, their efficacy against DOX-resistant MCF-7 BC cells was limited to transient thermal damage under AMF, highlighting the need for optimized combinatorial strategies in MDR scenarios.

Further advancing this paradigm, Chen *et al.*[234] developed a triple-action PCL-based IDDS incorporating MNPs, DOX, and the heat shock protein inhibitor 17-allylamino-17-demethoxygeldanamycin (17AAG) (Fig. 9C). Under AMF, MNPs produced photothermal effects to induce apoptosis, while 17AAG suppressed thermotolerance by blocking HSP90 activity. This synergistic approach—combining hyperthermia, chemotherapy, and molecular targeting—significantly enhanced anticancer efficacy in MCF-7 cells, establishing a robust platform for localized BC therapy.

4.2.3. Electro-responsive IDDS. Electro-responsive nanomaterials, typically composed of polyelectrolytes, undergo reversible volumetric changes through electric field modulation, enabling programmable structural transitions.[235] Incorporating polyelectrolyte particles with abundant ionizable groups into DDS confers dynamic responsiveness to electrical stimuli *via* contraction–expansion mechanisms.[236] Under external electric field stimulation, electro-responsive DDS achieve spatiotemporally controlled drug release profiles, including sustained, pulsatile, or on-demand delivery modes.[237,238] The high surface-to-volume ratio of nanoparticles further enhances drug-loading capacity and release sensitivity under electrical actuation.[239]

The therapeutic efficacy of catalytic cancer therapy remains constrained by inefficient ROS generation. Zheng *et al.*[240] engineered a self-powered triboelectric nanogenerator (TENG)-driven system for synergistic catalytic-chemotherapeutic intervention. This platform integrates graphitic carbon nitride ($g\text{-}C_3N_4$) nanosheets and DOX within biodegradable Gel/PCL nanofiber patches. Electric field stimulation amplified $g\text{-}C_3N_4$-mediated hydroxyl radical ($^{\bullet}OH$) production by 4.12-fold while enabling localized DOX release. Both *in vitro* and *in vivo* studies validated the TENG-powered system's capacity to significantly enhance tumor suppression through coupled catalytic-chemotherapeutic action.

Puiggalí-Jou *et al.*[241] fabricated electrospun PCL fibers co-loaded with poly(3,4-ethylenedioxythiophene) nanoparticles (PEDOT NPs) and Cur (Fig. 10). Spontaneous CUR diffusion from PCL fibers proved kinetically limited, necessitating electrical stimulation for controlled release. Upon application of voltage pulses, PEDOT NPs exhibited electromechanical actuation—expanding by 17% in diameter and migrating toward fiber surfaces—thereby inducing structural reorganization of the PCL matrix to accelerate CUR elution. Cumulative drug release correlated positively with pulse frequency, while post-

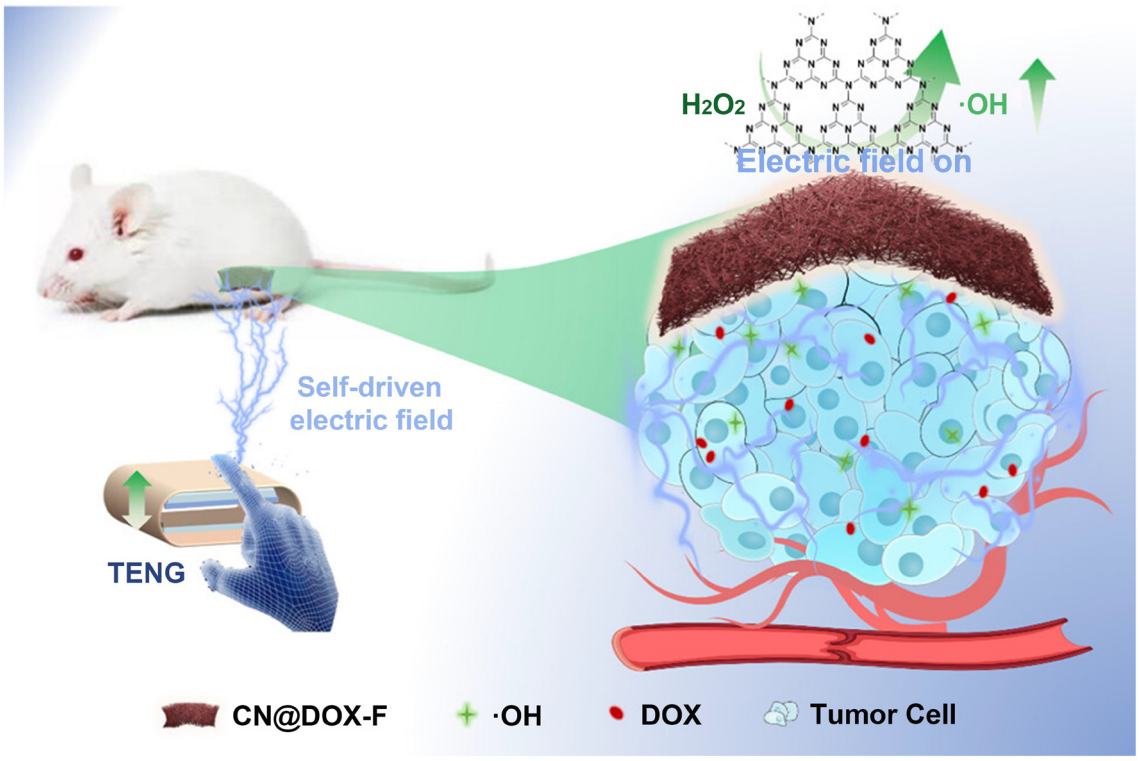

Fig. 10 Research on an electro-responsive IDDS: an autonomous platform integrating a triboelectric nanogenerator (TENG) with implantable Gel/PCL nanofibers for enhanced tumor suppression *via* electric field stimulation. Reproduced from ref. 241 with permission from American Chemical Society, copyright 2018.[241]

electrospinning CUR retained its anticancer bioactivity in cell-based assays.

4.3. Multi-stimuli-responsive IDDS

The integration of multiple triggering mechanisms enables precise spatiotemporal control over stimulation parameters, thereby enhancing the accuracy and flexibility of drug release profiles. Recent advancements in intelligent DDS have driven the development of multi-stimuli-responsive platforms for BC treatment, where endogenous (*e.g.*, pH, enzymes) and exogenous (*e.g.*, light, electric fields) stimuli are synergistically exploited. Unlike single-stimulus systems, multi-responsive DDS integrate distinct activation modalities on a unified nanoplatform, enabling programmable multi-stage drug release, co-delivery of therapeutic agents, and reversal of MDR through combinatorial therapeutic strategies.[242]

Polypyrrole (PPy), exhibiting dual pH/NIR responsiveness, was employed by Tiwari *et al.*[243] to functionalize electrospun PCL fibers loaded with PTX (Fig. 11A). Under NIR irradiation, PPy-coated matrices demonstrated enhanced anticancer efficacy at pH 5.5 compared to physiological pH 7.4, with PTX release kinetics dynamically modulated by light exposure. This

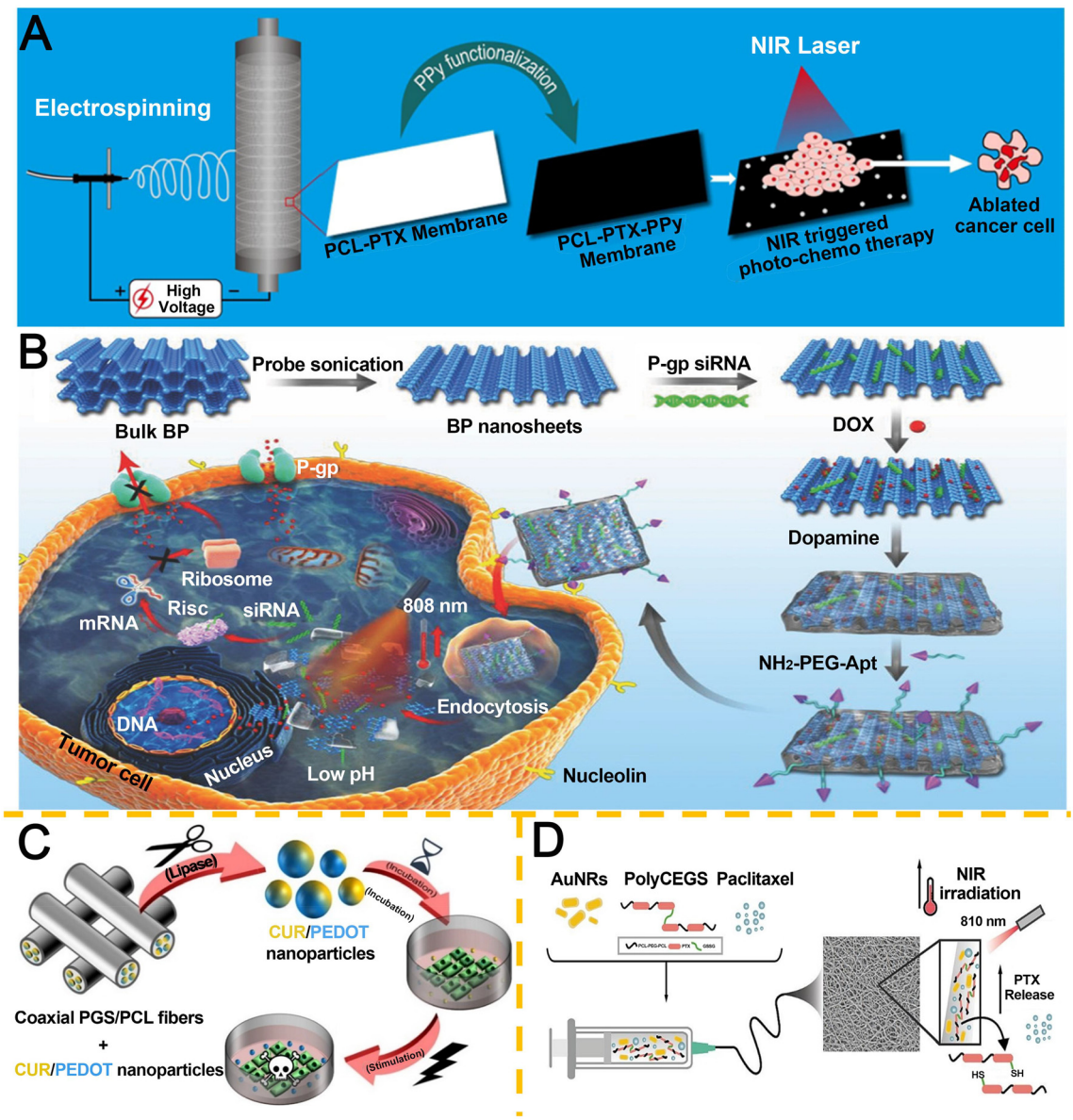

Fig. 11 Research on multi-responsive electrospun nanofiber-based IDDS. A. PPy-PCL-PTX nanofibrous membranes for NIR-activated photothermal ablation. Reproduced from ref. 243 with permission from American Chemical Society, copyright 2018.[243] B. PDA-BP hybrid nanosystems for pH/NIR-dual responsive chemo-gene-photothermal therapy. Reproduced from ref. 244 with permission from Wiley, copyright 2018.[244] C. Coaxial electrospun PGS/PCL core–shell fibers with enzyme-responsive and electroconductive (PEDOT) properties. Reproduced from ref. 246 with permission from Elsevier, copyright 2024.[246] D. PolyCEGS–AuNRs–PTX scaffolds with NIR-modulated release for spatiotemporal chemo-photothermal therapy. Reproduced from ref. 247 with permission from Elsevier, copyright 2025.[247]

Table 5 Recent advances in stimulus-actuated electrospun nanofiber-based IDDS for localized BC therapy

Classification	Nanomaterial	Drug	Polymer	Constructure	Therapy	Ref.
pH	—	Ellagic acid (EA)	Chitin (Ch)	—	Chemotherapy	248
	Sodium bicarbonate (SB)	DOX	PLLA	—	Chemotherapy	249
NIR	AuNPs/PDA	—	PCL	Core–shell	Photothermal therapy	250
	nRGO/AuNPs	—	PCL	—	Photothermal therapy	251
	AuNRs	—	PEG/PLGA/PLA	—	Photothermal therapy	252
	MWCNT	DOX	PLLA	—	Photothermal therapy/ chemotherapy	253
	GO	—	PCL	—	Photothermal therapy	254
	Au/poly (NIPAAm-*co*-NMA)	DOX/CUR	poly(NIPAAm-*co*-NMA)/PVA	Core–sheath	Photothermal therapy/ chemotherapy	255
AMF	IONP	BTZ	p(MMA-*co*-DMA)	—	Photothermal therapy/ chemotherapy	256
	Superparamagnetic graphene oxide (SPGO)	DOX	PU	—	Photothermal therapy/ chemotherapy	257
	Au	PTX/5-FU	PCL-Diol-*b*-PU/ PNIPAAm-*g*-CS	—	Photothermal therapy/ chemotherapy	258
	IONP	BTZ	PLGA	—	Photothermal therapy/ chemotherapy	259
	MNP	PTX	—	—	Photothermal therapy/ chemotherapy	260
pH + EMF	Nickel ferrite	DOX	CMC/PVA/PCL	Core–sheath	Photothermal therapy/ chemotherapy	261
pH + AMF	IONP/ammonium bicarbonate	DOX	PCL	—	Photothermal therapy/ chemotherapy	262
pH + ROS	DOX-ds/PUU	—	PU	—	Chemotherapy	263

dual-triggered system achieved site-specific drug delivery by coupling tumor microenvironment acidity with external photothermal activation.

Zeng *et al.*[244] engineered a multifunctional platform based on PDA-modified black phosphorus (BP) nanosheets (Fig. 11B). The PDA-BP hybrid exhibited superior stability and photothermal performance relative to bare BP. pH-Dependent drug release coupled with NIR-triggered payload liberation enabled effective co-delivery of P-glycoprotein siRNA and DOX, significantly suppressing drug efflux mechanisms. Cellular uptake assays confirmed tumor-selective targeting, while *in vitro* and *in vivo* studies demonstrated synergistic inhibition of tumor proliferation through multimodal therapeutic action.

Electroconductive polymers (ECPs), capable of redox-state transitions under electrical stimulation, represent promising candidates for designing on-demand drug release systems through conformational switching.[245] Expanding this paradigm, Resina *et al.*[246] fabricated coaxial electrospun poly(glycerol sebacate) (PGS)/PCL fibers encapsulating Cur-loaded poly(3,4-ethylenedioxythiophene) nanoparticles (CUR/PEDOT-NPs) (Fig. 11C). This dual-responsive system synergized endogenous enzymatic activation for sustained nanocarrier release with externally triggered electro-responsive drug liberation. The enzymatic sensitivity enabled long-term therapeutic action as implantable or transdermal devices, while electrical stimulation permitted precision-controlled anticancer payload delivery through PEDOT NP-mediated electromechanical actuation. Martorana *et al.*[247] developed polyurethane urea (PUU) electrospun membranes containing AuNRs and PTX by leveraging the redox responsiveness of glutathione-extended polyurethane urea (PolyCEGS) and the photo-responsiveness of AuNRs (Fig. 11D); when exposed to 3 W cm^{-2} NIR (810 nm), the temperature rose to 42.5 °C, and the fibers exhibited sustained PTX release—15% over 30 days and nearly 1.8 times more in simulated reducing conditions. Their outstanding photothermal effect and NIR light-triggered release resulted in significant synergistic cytotoxicity in the MCF-7 cell line. This system holds promise for achieving controlled, localized PTX release at tumor sites post-surgery, preventing recurrence and enhancing cytotoxicity through the combined effects of drug delivery and photothermal therapy, highlighting its potential for future cancer treatments.

Recent advances in stimulus-actuated electrospun nanofiber-based IDDS for localized BC therapy are systematically cataloged in Table 5.

5. Conclusion

Breast cancer incidence continues to rise globally, posing a critical threat to women's health. While advancements in multimodal therapeutic strategies have improved patient survival rates, treatment-related sequelae and systemic toxicities significantly compromise long-term quality of life and clinical outcomes. In recent years, electrospun nanofibers have emerged as a transformative platform for localized breast cancer therapy, demonstrating unparalleled advantages in controlled drug release, post-surgical subcutaneous implantation, and microenvironment-responsive functionality.

Current research has successfully integrated natural compounds (*e.g.*, PTX, Cur) with chemotherapeutics (*e.g.*, DOX, 5-FU) into electrospun systems, leveraging synergistic effects to

reduce systemic toxicity while enhancing tumor targeting.[170,172] However, the clinical translation of phytochemicals such as curcumin and piperine remains constrained by poor aqueous solubility and stability, necessitating nanoencapsulation or chemical functionalization to improve drug-loading efficiency. Furthermore, emerging targeted agents (*e.g.*, CDK4/6 inhibitors, PARP inhibitors) and immunotherapeutics (*e.g.*, *PD-1*/*PD-L1* antibodies) have yet to be widely incorporated into electrospun carriers, limiting the integration of IDDS with precision oncology paradigms. Recent innovations, such as photothermal electrospun nanofibers capable of delivering siRNA to immune cells for *PD-1* suppression and enhanced tumoricidal activity, highlight promising avenues for combining immunotherapy with nanofiber-mediated delivery,[264] combinations such as cytokines with PD-1/PD-L1 inhibitors potentiate local immune activation and reduce systemic toxicity, offering a superior therapeutic profile.[265] Future designs could exploit "drug-antibody co-loaded fibers" to amplify targeting specificity *via* localized retention effects while mitigating immune-related adverse events.[266]

On the other hand, current research on stimuli-responsive electrospun nanofiber IDDS predominantly focuses on pH-, light-, magnetic-, and electric-field-triggered mechanisms, while strategies leveraging endogenous cues such as mechanical stress (*e.g.*, tumor tissue contraction), enzyme activity (*e.g.*, matrix metalloproteinases, MMPs), or redox gradients (*e.g.*, elevated ROS) remain underexplored. For instance, ROS-scavenging electrospun fibers—capable of modulating oxidative stress within the tumor microenvironment—have yet to be fully harnessed in breast cancer therapy.[267] A critical frontier lies in designing multistimulus-integrated smart systems to achieve spatiotemporally precise drug release. Examples include dual-responsive "enzyme-photo" fibers that degrade *via* MMP-triggered cleavage in the tumor niche while enabling NIR-controlled payload release.[268] However, integrating drugs with stimuli-responsive materials necessitates balancing drug-loading efficiency with biocompatibility, and the inherent complexity of orchestrating sequential or concurrent stimulus-actuated mechanisms poses significant engineering challenges.

When integrating the aforementioned therapeutic agents and responsive systems to construct advanced treatment platforms, it is imperative to critically evaluate both the supporting capacity and inherent limitations of electrospun nanofibers for multimodal combination therapies. The application of electrospun nanofiber platforms for advanced multimodal therapy, despite enabling spatiotemporally controlled co-delivery of chemotherapeutic agents, natural products, immunomodulators, and gene vectors for synergy (*e.g.*, *via* cGAS-STING activation), is constrained by several factors. Major limitations involve the formidable challenge of compatible loading and independent release control for drugs with divergent properties (*e.g.*, hydrophilic siRNA *vs.* hydrophobic chemotherapeutics);[269] their typically lower gene transfection efficiency compared to specialized vectors, largely due to limited endosomal escape;[270] and the finite penetration depth of released drugs from the local implant into solid tumor tissue, which can impair the uniform distribution and efficacy of macromolecular agents like antibodies or checkpoint inhibitors.[269]

In summary, although electrospun nanofibers have advanced research in localized implantable drug delivery for BC through innovative drug-loading strategies and smart materials, its clinical translation remains constrained by several bottlenecks related to drug selection, systemic functional complexity, and manufacturing/quality control. At the manufacturing level, future research must move beyond merely acknowledging issues like "poor reproducibility and difficult scaling" and instead actively explore emerging solutions compliant with Good Manufacturing Practice (GMP). These include needle-free continuous electrospinning platforms for stable scale-up production and the systematic evaluation of safer alternatives to organic solvents, such as aqueous solvent systems. Only through such in-depth exploration oriented toward industrialization and clinical compliance can this technology be propelled toward practical application.

6. Future perspectives

The rapid convergence of advanced technologies continues to inspire transformative innovations in breast cancer therapy. Future research on electrospun nanofiber-based IDDS should prioritize breakthroughs across five strategic domains:

(1) Synergistic drug-carrier innovations

Future efforts should focus on integrating electrospun nanofibers with antibody–drug conjugates (ADCs) and gene therapy vectors, leveraging their high surface area-to-volume ratio for stable macromolecular drug loading and sustained release. Pioneering the development of "drug-carrier functional integration" materials—such as fibers combining drug delivery with photothermal conversion capabilities—could transcend the passive carrier paradigm, enabling multifunctional therapeutic platforms. Given the established clinical foundation of biologics such as ADCs, such synergistic systems are anticipated to enter clinical evaluation within 5–8 years.

Electrospun nanofibers can be endowed with a series of multi-chamber inner structures,[271,272] such as core–sheath,[273] Janus,[274] tri-chamber core–sheath,[275] tri-chamber Janus,[276] and a combination of Janus and core–sheath.[277–279] These complex nanostructures can support a strong platform for tailoring components, compositions and their spatial distribution.[280–282] Based on their applications, various distinct process–structure–performance relationships can be disclosed for promoting abundant synergistic drug-carrier innovations.

(2) Multi-stimulus-responsive system engineering

Next-generation systems should employ "endogenous-exogenous dual-actuation" logic (*e.g.*, ROS/pH-responsive mechanisms coupled with near-infrared triggering) to achieve orthogonal stimulus-controlled cascading drug release. This represents one of the most promising clinical translation pathways. Its core principle lies in leveraging endogenous signals

for targeted localization, followed by the application of exogenous stimuli to achieve precise, on-demand release. It is anticipated that proof-of-concept will be completed in preclinical models within 3–5 years. Concurrent development of novel responsive materials (*e.g.*, piezoelectric polymers, sonosensitizers) is critical to address diverse tumor microenvironmental features, including hypoxia and elevated ATP levels.

(3) Multimodal IDDS convergence

Strategic integration with bioimaging technologies could enable intraoperative precision implantation and postoperative therapeutic monitoring *via* contrast-enhanced visualization. Combining 3D bioprinting with electrospinning[283,284] allows fabrication of patient-specific porous scaffolds that anatomically conform to post-resection cavities, mimic mammary tissue mechanics, and enable gradient drug release. Synergy with immunotherapy could be achieved by co-loading immune checkpoint inhibitors and tumor antigens to activate localized antitumor immunity.[285] Among these, the integration with immunotherapy and the use of 3D-printed personalized scaffolds are regarded as key mid- to long-term (approximately 5–10 years) directions with potential to transform clinical practice.

(4) Clinical translation roadmap

Postoperative IDDS must balance initial mechanical support (elastic modulus matching breast tissue) with long-term biodegradability (eliminating secondary extraction surgeries). This demands biocompatible polymer matrices with tunable copolymer ratios to synchronize degradation kinetics and mechanical performance. Standardized preclinical models —including organoid platforms and humanized murine systems—are essential to accelerate FDA/EMA approvals. It is recommended that translational research be divided into two distinct phases: the next three years should focus on establishing GMP-compliant standardized production processes and aqueous electrospinning systems, while the subsequent 3–5 years should be dedicated to conducting first-in-human clinical trials to evaluate safety and preliminary efficacy. Addressing current manufacturing limitations requires continuous electrospinning systems for GMP-compliant production, rigorous quality control metrics (drug distribution homogeneity, batch-to-batch release consistency), and transition to aqueous electrospinning to replace toxic organic solvents, ensuring both biocompatibility and environmental sustainability.

(5) Personalized therapy and sustainable development

Tailoring fiber-drug regimens to breast cancer subtypes (*e.g.*, *HER2*-positive, triple-negative) is imperative. For *HER2*-positive cases, surface functionalization with trastuzumab could enhance tumor targeting. Real-time therapeutic monitoring may integrate fluorescence markers or MRI contrast agents (*e.g.*, superparamagnetic iron oxide nanoparticles) into fibers for imaging-guided treatment assessment. The mature application of personalized treatment regimens is projected to require approximately 10 years, ultimately depending on the establishment of a "design-manufacture-verify" closed-loop framework.

Achieving the ultimate goal of "precision implantation, on-demand therapeutic delivery" necessitates multidisciplinary collaboration among material scientists, clinicians, and biomedical engineers to harmonize technological innovation with clinical practicality.

Conflicts of interest

There are no conflicts to declare.

Abbreviations

17AAG	17-Allylamino-17-demethoxygeldanamycin
5-FU	5-Fluorouracil
AgNP	Silver nanoparticles
AGS	Alginate/gelatin sponge
AMF	Alternating magnetic field
AMG	Amygdalin
Apa	Apatinib
Art	Artemisinin
ASA	Aspirin
ATRA	All-trans retinoic acid
AuNPs	Gold nanoparticles
AuNRs	Gold nanorods
BC	Breast cancer
BHC	Berberine hydrochloride
BP	Black phosphorus
CA	Citric acid
Coll	Collagen
CPT	Chemo-photothermal therapy
CS	Chitosan
CSCs	Cancer stem cells
Cur	Curcumin
DCIS	Ductal carcinoma *in situ*
DDS	Drug delivery systems
DMSO	Dimethyl sulfoxide
DOX	Doxorubicin
DOX·HCl	DOX hydrochloride
DSF	Disulfiram
DTX	Docetaxel
EC	Ethyl cellulose
ECPs	Electroconductive polymers
EPR	Enhanced permeability and retention
FA	Folate
Gel	Gelatin
GMP	Good manufacturing practice
HAP	Hydroxyapatite
IDDS	Implantable drug delivery systems
IONC	Magnetic iron oxide nanocubes synthesis
IPNs	Interpenetrating polymer networks
ISL	Isoorientin-loaded
MC	Methylcellulose
MDR	Multidrug resistance
MNA	Metronidazole

MNPs	Magnetic nanoparticles
MSNs	Mesoporous silica nanoparticles
MWCNTs	Multi-walled carbon nanotubes
NIR	Near infrared
PBS	Physiological conditions
PCL	Polycaprolactone
PDA	Polydopamine
PEG	Polyethylene glycol
PEI	Polyethyleneimine
PG	Prodigiosin
PGS	Poly(glycerol sebacate)
PHBV	Poly(3-hydroxybutyrate-*co*-3-hydroxyvalerate)
PIP	Piperine
PLA	Poly (lactic acid)
PLEO	Pistacia lentiscus essential oil
PLGA	Poly(D,L-lactide-*co*-glycolide)
PPy	Polypyrrole
PTX	Paclitaxel
PUU	Polyurethane urea
PVP	Polyvinylpyrrolidone
Que	Quercetin
RES	Resveratrol
rGO	Graphene oxide
ROS	Reactive oxygen species
SF	Silk fibroin
SRDDS	Stimuli-responsive drug delivery systems (SRDDS)
SV	Simvastatin
TENG	Triboelectric nanogenerator
TMX	Tamoxifen
TNBC	Triple-negative breast cancer

Data availability

This review is based on previously published studies. No new primary data were generated for this article and all images cited herein have obtained image copyright permissions. The data supporting the findings of this review were derived from the sources cited in the references, which are publicly available through their respective DOIs, PubMed/Medline, or other academic databases.

References

1 R. L. Siegel, T. B. Kratzer, A. N. Giaquinto, H. Sung and A. Jemal, *CA-Cancer J. Clin.*, 2025, **75**, 10–45.
2 O. Ginsburg, C.-H. Yip, A. Brooks, A. Cabanes, M. Caleffi, J. A. D. Yataco, B. Gyawali, V. McCormack, M. McLaughlin de Anderson, R. Mehrotra, A. Mohar, R. Murillo, L. E. Pace, E. D. Paskett, A. Romanoff, A. F. Rositch, J. R. Scheel, M. Schneidman, K. Unger-Saldaña, V. Vanderpuye, T.-Y. Wu, S. Yuma, A. Dvaladze, C. Duggan and B. O. Anderson, *Cancer*, 2020, **126**, 2379–2393.
3 T. Sinha, *Int. J. Cancer Ther. Oncol.*, 2018, **10**, 555790, DOI: 10.19080/CTOIJ.2018.10.555790.
4 B. MacMahon, P. Cole and J. Brown, *J. Natl. Cancer Inst.*, 1973, **50**, 21–42.
5 A. Burguin, C. Diorio and F. Durocher, *J. Pers. Med.*, 2021, **11**, 808.
6 D. Kingsmore, D. Hole and C. Gillis, *Br. J. Cancer*, 2004, **90**, 1920–1925.
7 S. K. Down, P. K. Jha, A. Burger and M. I. Hussien, *Breast J.*, 2013, **19**, 56–63.
8 H. J. Burstein, G. Curigliano, B. Thürlimann, *et al.*, *Ann. Oncol.*, 2021, **32**, 1216–1235.
9 Y. Qu, B. Y. Chu, J. R. Peng, J. F. Liao, T. T. Qi, K. Shi, X. N. Zhang, Y. Q. Wei and Z. Y. Qian, *NPG Asia Mater.*, 2015, **7**, e207.
10 A. K. Azab, J. Kleinstern, V. Doviner, B. Orkin, M. Srebnik, A. Nissan and A. Rubinstein, *J. Controlled Release*, 2007, **123**, 116–122.
11 J. E. Belz, R. Kumar, P. Baldwin, N. C. Ojo, A. S. Leal, D. B. Royce, D. Zhang, A. L. van de Ven, K. T. Liby and S. Sridhar, *Theranostics*, 2017, **7**, 4340–4349.
12 V. Jain, H. Kumar, H. V. Anod, P. Chand, N. V. Gupta, S. Dey and S. S. Kesharwani, *J. Controlled Release*, 2020, **326**, 628–647.
13 M. Nikolova, R. Slavchov and G. Nikolova, in *Drug Discovery and Evaluation: Methods in Clinical Pharmacology*, Springer, Cham, 2020, pp. 533–546.
14 Z. Mirza and S. Karim, *Semin. Cancer Biol.*, 2021, **69**, 226–237.
15 S. Chen, W. Yao, H. Wang, T. Wang, X. Xiao, G. Sun, J. Yang, Y. Guan, Z. Zhang, Z. Xia, M. Li, Y. Tao and Z. Hei, *Theranostics*, 2022, **12**, 4904–4921.
16 S. Chen, W. Yao, Z. Ding, J. Du, T. Wang, X. Xiao, L. Zhang, J. Yang, Y. Guan, C. Chen, Y. Tao, M. Li, H. Wang and Z. Hei, *Adv. Fiber Mater.*, 2024, **6**, 1428–1445.
17 K. Baylón, P. Rodríguez-Camarillo, A. Elías-Zúñiga, J. A. Díaz-Elizondo, R. Gilkerson and K. Lozano, *Membranes*, 2017, **7**, 47.
18 D.-G. Yu, T. Chen and C. He, *Curr. Drug Delivery*, 2026, **23**, 242.
19 N. Desai, M. Momin, T. Khan, S. Gharat, R. S. Ningthoujam and A. Omri, *Expert Opin. Drug Delivery*, 2021, **18**, 1261–1290.
20 V. Chandrakala, V. Aruna and G. Angajala, *Emergent Mater.*, 2022, **5**, 1593–1615.
21 N. Mamidi, R. M. V. Delgadillo, A. O. Sustaita, K. Lozano and M. M. Yallapu, *Med. Res. Rev.*, 2025, **45**, 576–628.
22 K. E. Broaders, S. Grandhe and J. M. J. Fréchet, *J. Am. Chem. Soc.*, 2011, **133**, 756–758.
23 R. Chelliah, M. Rubab, S. Vijayalakshmi, M. Karuvelan, K. Barathikannan and D.-H. Oh, *Next Nanotechnol.*, 2025, **8**, 100209.
24 P. P. Deshpande, S. Biswas and V. P. Torchilin, *Nanomedicine*, 2013, **8**, 1509–1528.
25 Y.-J. Hu, R.-J. Ju, F. Zeng, X.-R. Qi and W.-L. Lu, *Biomater. Eng.*, 2021, pp. 3–24.
26 S. Kotta, H. M. Aldawsari, S. M. Badr-Eldin, A. B. Nair and K. Yt, *Pharmaceutics*, 2022, **14**, 1636.

27 B. Ghosh and S. Biswas, *J. Controlled Release*, 2021, **332**, 127–147.
28 I. Negut and B. Bita, *Pharmaceutics*, 2023, **15**, 976.
29 M. Sepantafar, R. Maheronnaghsh, H. Mohammadi, F. Radmanesh, M. M. Hasani-sadrabadi, M. Ebrahimi and H. Baharvand, *Trends Biotechnol.*, 2017, **35**, 1074–1087.
30 X. Li, X. Xu, M. Xu, Z. Geng, P. Ji and Y. Liu, *Front. Bioeng. Biotechnol.*, 2023, **11**, DOI: 10.3389/fbioe.2023.1140436.
31 J. Han, T. Sheng, Y. Zhang, H. Cheng, J. Gao, J. Yu and Z. Gu, *Adv. Mater.*, 2024, **36**, 2209778.
32 Z. Zhang, C. He and X. Chen, *Adv. Mater.*, 2024, **36**, 2308894.
33 B. Mishra, B. B. Patel and S. Tiwari, *Nanomedicine*, 2010, **6**, 9–24.
34 S. Bamrungsap, Z. Zhao, T. Chen, L. Wang, C. Li, T. Fu and W. Tan, *Nanomedicine*, 2012, **7**, 1253–1271.
35 R. C. Parida, D. Thamizhanban, K. Lakshmi and G. K. Jena, *Biomed. Mater. Devices*, 2025, DOI: 10.1007/s44174-025-00415-0.
36 M. A. Dobrovolskaia and S. E. McNeil, *Nat. Nanotechnol.*, 2007, **2**, 469–478.
37 B. Balusamy, A. Celebioglu, A. Senthamizhan and T. Uyar, *J. Controlled Release*, 2020, **326**, 482–509.
38 L. Li, R. Hao, J. Qin, J. Song, X. Chen, F. Rao, J. Zhai, Y. Zhao, L. Zhang and J. Xue, *Adv. Fiber Mater.*, 2022, **4**, 1375–1413.
39 A. Valizadeh, S. Asghari, S. Abbaspoor, A. Jafari, M. Raeisi and Y. Pilehvar, *Wiley Interdiscip. Rev.: Nanomed. Nanobiotechnol.*, 2023, **15**, e1909.
40 S. Chaturvedi, V. Rastogi and M. Kumar, *J. Drug Delivery Sci. Technol.*, 2024, **93**, 105447.
41 N. Kimizuka, *Adv. Polym. Sci*, 2008, pp. 1–26.
42 G. Che, B. B. Lakshmi, C. R. Martin, E. R. Fisher and R. S. Ruoff, *Chem. Mater.*, 1998, **10**, 260–267.
43 J. Zhao, W. Han, H. Chen, M. Tu, R. Zeng, Y. Shi, Z. Cha and C. Zhou, *Carbohydr. Polym.*, 2011, **83**, 1541–1546.
44 C. Jia, L. Li, J. Song, Z. Li and H. Wu, *Acc. Mater. Res.*, 2021, **2**, 432–446.
45 J. Carriles, P. Nguewa and G. González-Gaitano, *Int. J. Mol. Sci.*, 2023, **24**, 14757.
46 A. Greiner and J. H. Wendorff, *Angew. Chem., Int. Ed.*, 2007, **46**, 5670–5703.
47 N. Bhardwaj and S. C. Kundu, *Biotechnol. Adv.*, 2010, **28**, 325–347.
48 W. Lu, J. Sun and X. Jiang, *J. Mater. Chem.*, 2014, **2**, 2369–2380.
49 G. Yang, X. Li, Y. He, J. Ma, G. Ni and S. Zhou, *Prog. Polym. Sci.*, 2018, **81**, 80–113.
50 Y. Ding, W. Li, F. Zhang, Z. Liu, N. Z. Ezazi, D. Liu and H. A. Santos, *Adv. Funct. Mater.*, 2019, **29**, 1802852.
51 M. Khodadadi, S. Alijani, M. Montazeri, N. Esmaeilizadeh, S. Sadeghi-Soureh and Y. Pilehvar-Soltanahmadi, *J. Biomed. Mater. Res., Part A*, 2020, **108**, 1444–1458.
52 J. Zhao and W. Cui, *Adv. Fiber Mater.*, 2020, **2**, 229–245.
53 N. Mamidi, A. E. Zuníga and J. Villela-Castrejón, *Mater. Sci. Eng., C*, 2020, **112**, 110928.
54 C. Huang, S. J. Soenen, J. Rejman, B. Lucas, K. Braeckmans, J. Demeester and S. C. D. Smedt, *Chem. Soc. Rev.*, 2011, **40**, 2417–2434.
55 Y. Fu, X. Li, Z. Ren, C. Mao and G. Han, *Small*, 2018, **14**, 1801183.
56 N. Fomina, J. Sankaranarayanan and A. Almutairi, *Adv. Drug Delivery Rev.*, 2012, **64**, 1005–1020.
57 S. Mura, J. Nicolas and P. Couvreur, *Nat. Mater.*, 2013, **12**, 991–1003.
58 Y. Li, K. Xiao, W. Zhu, W. Deng and K. S. Lam, *Adv. Drug Delivery Rev.*, 2014, **66**, 58–73.
59 A. Ullah, Y. Saito, S. Ullah, Md. K. Haider, H. Nawaz, P. Duy-Nam, D. Kharaghani and I. S. Kim, *Int. J. Biol. Macromol.*, 2021, **166**, 1009–1021.
60 J. Xue, J. Xie, W. Liu and Y. Xia, *Acc. Chem. Res.*, 2017, **50**, 1976–1987.
61 S. Thenmozhi, N. Dharmaraj, K. Kadirvelu and H. Y. Kim, *Mater. Sci. Eng., B*, 2017, **217**, 36–48.
62 F. Anton, *US Patent*, 2160962, 1944.
63 D. H. Reneker and I. Chun, *Nanotechnology*, 1996, **7**, 216.
64 D. H. Reneker, A. L. Yarin, H. Fong and S. Koombhongse, *J. Appl. Phys.*, 2000, **87**, 4531–4547.
65 H. Dai, J. Gong, H. Kim and D. Lee, *Nanotechnology*, 2002, **13**, 674–677.
66 N. Mamidi, *et al.*, *ACS Biomater. Sci. Eng.*, 2022, **8**(9), 3690–3716.
67 M. Rahmati, D. K. Mills, A. M. Urbanska, M. R. Saeb, J. R. Venugopal, S. Ramakrishna and M. Mozafari, *Prog. Mater. Sci.*, 2021, **117**, 100721.
68 S. Kang, K. Zhao, D.-G. Yu, X. Zheng and C. Huang, *Adv. Fiber Mater.*, 2022, **4**, 404–435.
69 T. S. M. Kumar, K. S. Kumar, N. Rajini, S. Siengchin, N. Ayrilmis and A. V. Rajulu, *Composites, Part B*, 2019, **175**, 107074.
70 Y. Yan, X. Liu, J. Yan, C. Guan and J. Wang, *Energy Environ. Mater.*, 2021, **4**, 502–521.
71 D.-M. Xie, Q. Zhong, X. Xu, Y. Li, S. Chen, M. Li and C. Peng, *Int. J. Pharm.*, 2023, **632**, 122581.
72 A. J. Robinson, A. Pérez-Nava, S. C. Ali, J. B. González-Campos, J. L. Holloway and E. M. Cosgriff-Hernandez, *Matter*, 2021, **4**, 821–844.
73 D.-J. Sun, W.-Z. Song, C.-L. Li, T. Chen, D.-S. Zhang, J. Zhang, S. Ramakrishna and Y.-Z. Long, *Nano Energy*, 2022, **101**, 107599.
74 M. Sivan, D. Madheswaran, J. Valtera, E. K. Kostakova and D. Lukas, *Mater. Des.*, 2022, **213**, 110308.
75 A. Balogh, B. Farkas, G. Verreck, J. Mensch, E. Borbás, B. Nagy, G. Marosi and Z. K. Nagy, *Int. J. Pharm.*, 2016, **505**, 159–166.
76 D. Zong, X. Zhang, X. Yin, F. Wang, J. Yu, S. Zhang and B. Ding, *Adv. Fiber Mater.*, 2022, **4**, 1434–1462.
77 C. Cleeton, A. Keirouz, X. Chen and N. Radacsi, *ACS Biomater. Sci. Eng.*, 2019, **5**, 4183–4205.

78 G. I. Taylor, *Proc. R. Soc. London, Ser. A*, 1997, **280**, 383–397.
79 W. Guan, W. Zhou, J. Lu and C. Lu, *Chem. Soc. Rev.*, 2015, **44**, 6981–7009.
80 W. Jiang, P. Zhao, W. Song, M. Wang and D.-G. Yu, *Biomolecules*, 2022, **12**, 1110.
81 Y. Bai, Y. Liu, H. Lv, H. Shi, W. Zhou, Y. Liu and D.-G. Yu, *Polymers*, 2022, **14**, 4311.
82 V. Jacobs, R. D. Anandjiwala and M. Maaza, *J. Appl. Polym. Sci.*, 2010, **115**, 3130–3136.
83 X. Wen, J. Xiong, S. Lei, L. Wang and X. Qin, *Adv. Fiber Mater.*, 2022, **4**, 145–161.
84 J. Xue, T. Wu, Y. Dai and Y. Xia, *Chem. Rev.*, 2019, **119**(8), 5298–5415.
85 V. Beachley and X. Wen, *Mater. Sci. Eng., C*, 2009, **29**, 663–668.
86 J. M. Deitzel, J. Kleinmeyer, D. Harris and N. C. Beck Tan, *Polymer*, 2001, **42**, 261–272.
87 H. M. Ibrahim and A. Klingner, *Polym. Test.*, 2020, **90**, 106647.
88 D.-G. Yu, M. Wang, X. Li, X. Liu, L.-M. Zhu and S. W. Annie Bligh, *Wiley Interdiscip. Rev.: Nanomed. Nanobiotechnol.*, 2020, **12**, e1601.
89 X. Wang, T. You, W. Zheng, X. Li, S. Chen and F. Xu, *Chem. Eng. J.*, 2024, **483**, 148841.
90 S. C. Park, Y. Yuan, K. Choi, S.-O. Choi and J. Kim, *Materials*, 2018, **11**, 681.
91 L. R. Anderson, E. Noureen, S. R. Collinson, P. G. Taylor, G. C. Shearman, K. Rietdorf, K. N. White and N. P. Chatterton, *Int. J. Pharm.*, 2026, **687**, 126396.
92 Z. Sun, E. Zussman, A. l. Yarin, J. h. Wendorff and A. Greiner, *Adv. Mater.*, 2003, **15**, 1929–1932.
93 Y. Lu, J. Huang, G. Yu, R. Cardenas, S. Wei, E. K. Wujcik and Z. Guo, *Wiley Interdiscip. Rev.: Nanomed. Nanobiotechnol.*, 2016, **8**, 654–677.
94 T. Hai, X. Wan, D.-G. Yu, K. Wang, Y. Yang and Z.-P. Liu, *Mater. Des.*, 2019, **162**, 70–79.
95 C. Wang, K.-W. Yan, Y.-D. Lin and P. C. H. Hsieh, *Macromolecules*, 2010, **43**, 6389–6397.
96 M. Reise, S. Kranz, A. Guellmar, R. Wyrwa, T. Rosenbaum, J. Weisser, A. Jurke, M. Schnabelrauch, M. Heyder, D. C. Watts and B. W. Sigusch, *Dent. Mater.*, 2023, **39**, 132–139.
97 Y. Liu, X. Chen, Y. Liu, Y. Gao and P. Liu, *Polymers*, 2022, **14**, 469.
98 P. Gupta and G. L. Wilkes, *Polymers*, 2003, **44**, 6353–6359.
99 M. Wang, D. Li, J. Li, S. Li, Z. Chen, D.-G. Yu, Z. Liu and J. Z. Guo, *Mater. Des.*, 2020, **196**, 109075.
100 D. Li, M. Wang, W.-L. Song, D.-G. Yu and S. W. A. Bligh, *Biomolecules*, 2021, **11**, 635.
101 A. Amarjargal, O. Cegielska, D. Kolbuk, B. Kalaska and P. Sajkiewicz, *ACS Appl. Mater. Interfaces*, 2024, **16**, 153–165.
102 J. Zhou, Y. Chen, Y. Liu, T. Huang, J. Xing, R. Ge and D.-G. Yu, *Int. J. Biol. Macromol.*, 2024, **269**, 132113.
103 G. Kuang, Q. Zhang, Y. Yu, X. Ding, W. Sun, X. Shen and Y. Zhao, *Chem. Eng. J.*, 2023, **455**, 140619.
104 B.-S. Lee, S.-Y. Jeon, H. Park, G. Lee, H.-S. Yang and W.-R. Yu, *Sci. Rep.*, 2014, **4**, 6758.
105 G. H. Lee, J.-C. Song and K.-B. Yoon, *Macromol. Res.*, 2010, **18**, 571–576.
106 A. K. Moghe and B. S. Gupta, *Polym. Rev.*, 2008, **48**, 353–377.
107 M.-L. Wang, D.-G. Yu and S. W. A. Bligh, *Appl. Mater. Today*, 2023, **31**, 101766.
108 D.-G. Yu, J.-H. Yu, L. Chen, G. R. Williams and X. Wang, *Carbohydr. Polym.*, 2012, **90**, 1016–1023.
109 L. R. Anderson, E. Noureen, S. R. Collinson, P. G. Taylor, G. Shearman, K. Rietdorf, K. N. White and N. P. Chatterton, *Int. J. Pharm.*, 2025, **687**, 1–15.
110 Q. Zheng, Y. Xi and Y. Weng, *RSC Adv.*, 2024, **14**, 3359–3378.
111 M. Wang, J. Hou, D.-G. Yu, S. Li, J. Zhu and Z. Chen, *J. Alloys Compd.*, 2020, **846**, 156471.
112 P. Zhao, K. Zhou, Y. Xia, C. Qian, D.-G. Yu, Y. Xie and Y. Liao, *Adv. Fiber Mater.*, 2024, **6**, 1053–1073.
113 D.-G. Yu and J. Liu, *Curr. Drug Deliv.*, 2026, **23**, vi–vii.
114 D. Regan, A. Guth, J. Coy and S. Dow, *Vet. J.*, 2016, **207**, 20–28.
115 A. E. Giuliano, J. L. Connolly, S. B. Edge, E. A. Mittendorf, H. S. Rugo, L. J. Solin, D. L. Weaver, D. J. Winchester and G. N. Hortobagyi, *CA-Cancer J. Clin.*, 2017, **67**, 290–303.
116 Y. T. Lee, Y. J. Tan and C. E. Oon, *Eur. J. Pharmacol.*, 2018, **834**, 188–196.
117 K. E. Albinali, M. M. Zagho, Y. Deng and A. A. Elzatahry, *Int. J. Nanomed.*, 2019, **14**, 1707–1723.
118 W. J. Lesterhuis, J. B. A. G. Haanen and C. J. A. Punt, *Nat. Rev. Drug Discovery*, 2011, **10**, 591–600.
119 L. Milling, Y. Zhang and D. J. Irvine, *Adv. Drug Delivery Rev.*, 2017, **114**, 79–101.
120 T. N. Gide, C. Quek, A. M. Menzies, A. T. Tasker, P. Shang, J. Holst, J. Madore, S. Y. Lim, R. Velickovic, M. Wongchenko, Y. Yan, S. Lo, M. S. Carlino, A. Guminski, R. P. M. Saw, A. Pang, H. M. McGuire, U. Palendira, J. F. Thompson, H. Rizos, I. P. da Silva, M. Batten, R. A. Scolyer, G. V. Long and J. S. Wilmott, *Cancer Cell*, 2019, **35**, 238–255.
121 Z. Zhao, L. Zheng, W. Chen, W. Weng, J. Song and J. Ji, *J. Hematol. Oncol.*, 2019, **12**, 126.
122 Q. Chen, C. Wang, X. Zhang, G. Chen, Q. Hu, H. Li, J. Wang, D. Wen, Y. Zhang, Y. Lu, G. Yang, C. Jiang, J. Wang, G. Dotti and Z. Gu, *Nat. Nanotechnol.*, 2019, **14**, 89–97.
123 N. Vasan, J. Baselga and D. M. Hyman, *Nature*, 2019, **575**, 299–309.
124 J. B. Wolinsky, Y. L. Colson and M. W. Grinstaff, *J. Controlled Release*, 2012, **159**, 14–26.
125 Z. Chen, Z. Chen, A. Zhang, J. Hu, X. Wang and Z. Yang, *Biomater. Sci.*, 2016, **4**, 922–932.

126 S. Nobili, D. Lippi, E. Witort, M. Donnini, L. Bausi, E. Mini and S. Capaccioli, *Pharmacol. Res.*, 2009, **59**, 365–378.
127 S. Mitra and R. Dash, *J. Evidence-Based Complementary Altern. Med.*, 2018, **2018**, 8324696.
128 A. Arshi, S. M. Hosseini, F. S. K. Hosseini, Z. Y. Amiri, F. S. Hosseini, M. Sheikholia Lavasani, H. Kerdarian and M. S. Dehkordi, *Mol. Biol. Rep.*, 2019, **46**, 2059–2066.
129 S. A. Seyhan, D. B. Alkaya, S. Cesur and A. Sahin, *Int. J. Biol. Macromol.*, 2023, **239**, 124201.
130 M. A. Sheikh and C. S. Saini, *Food Biosci.*, 2022, **46**, 101467.
131 R. Pérez-Tomás, B. Montaner, E. Llagostera and V. Soto-Cerrato, *Biochem. Pharmacol.*, 2003, **66**, 1447–1452.
132 U. M. Akpan, M. Pellegrini, J. D. Obayemi, T. Ezenwafor, D. Browl, C. J. Ani, D. Yiporo, A. Salifu, S. Dozie-Nwachukwu, S. Odusanya, J. Freeman and W. O. Soboyejo, *Mater. Sci. Eng., C*, 2020, **114**, 110976.
133 A. E. Ring and P. A. Ellis, *Cancer Treat. Rev.*, 2005, **31**, 618–627.
134 M.-Y. Hsu, C.-H. Hsieh, Y.-T. Huang, S.-Y. Chu, C.-M. Chen, W.-J. Lee and S.-J. Liu, *Cancers*, 2021, **13**, 3350.
135 A. Niedzwiecki, M. W. Roomi, T. Kalinovsky and M. Rath, *Nutrients*, 2016, **8**, 552.
136 K. Chen, H. Pan, Z. Yan, Y. Li, D. Ji, K. Yun, Y. Su, D. Liu and W. Pan, *Int. J. Biol. Macromol.*, 2021, **182**, 1339–1350.
137 A. Thawabteh, S. Juma, M. Bader, D. Karaman, L. Scrano, S. A. Bufo and R. Karaman, *Toxins*, 2019, **11**, 656.
138 S. Jain, S. R. K. Meka and K. Chatterjee, *ACS Biomater. Sci. Eng.*, 2016, **2**, 1376–1385.
139 D. Babadi, S. Dadashzadeh, Z. Shahsavari, S. Shahhosseini, T. L. M. ten Hagen and A. Haeri, *Int. J. Pharm.*, 2022, **624**, 121990.
140 J. C. Merritt, S. D. Richbart, E. G. Moles, A. J. Cox, K. C. Brown, S. L. Miles, P. T. Finch, J. A. Hess, M. T. Tirona, M. A. Valentovic and P. Dasgupta, *Pharmacol. Ther.*, 2022, **238**, 108177.
141 A. R. Ahmady, A. Solouk, S. Saber-Samandari, S. Akbari, H. Ghanbari and B. E. Brycki, *J. Colloid Interface Sci.*, 2023, **638**, 616–628.
142 W. Ren, Z. Qiao, H. Wang, L. Zhu and L. Zhang, *Med. Res. Rev.*, 2003, **23**, 519–534.
143 K. Ganesan, F. Gao, C. Zheng, C. Xu, H. Tang, Y. Sui, C. Xie and J. Chen, *J. Drug Delivery Sci. Technol.*, 2024, **96**, 105609.
144 C. El-Baba, A. Baassiri, G. Kiriako, B. Dia, S. Fadlallah, S. Moodad and N. Darwiche, *Apoptosis*, 2021, **26**, 491–511.
145 M. Eslami Vaghar, M. Dadashpour, E. Derakhshan, V. Vahedian, S. A. Shahrtash, A. Firouzi Amandi, M. Eslami, M. Hasannia, Z. Mehrabi and L. Roshangar, *Cancer Nano*, 2024, **15**, 58.
146 S. Sharmin, Md. M. Rahaman, M. Martorell, J. Sastre-Serra, J. Sharifi-Rad, M. Butnariu, I. C. Bagiu, R. V. Bagiu and M. T. Islam, *Cancer Cell Int.*, 2021, **21**, 612.
147 K. Nurgali, R. T. Jagoe and R. Abalo, *Front. Pharmacol.*, 2018, **9**, DOI: 10.3389/fphar.2018.00245.
148 M. Khodadadi, S. Alijani, M. Montazeri, N. Esmaeilizadeh, S. Sadeghi-Soureh and Y. Pilehvar-Soltanahmadi, *J. Biomed. Mater. Res., Part A*, 2020, **108**, 1444–1458.
149 Y. Hu, Y. Xu, R. L. Mintz, X. Luo, Y. Fang, Y.-H. Lao, H. F. Chan, K. Li, S. Lv, G. Chen, Y. Tao, Y. Luo and M. Li, *Biomaterials*, 2023, **293**, 121942.
150 B. Bhattacharya and S. Mukherjee, *J. Cancer Ther.*, 2015, **06**, 849.
151 G. Yang, J. Wang, Y. Wang, L. Li, X. Guo and S. Zhou, *ACS Nano*, 2015, **9**, 1161–1174.
152 X. Li, F. Xu, Y. He, Y. Li, J. Hou, G. Yang and S. Zhou, *Adv. Funct. Mater.*, 2020, **30**, 2004851.
153 J. Li, J. Li, Y. Yao, T. Yong, N. Bie, Z. Wei, X. Li, S. Li, J. Qin, H. Jia, Q. Du, X. Yang and L. Gan, *Theranostics*, 2022, **12**, 3503–3517.
154 X. Li, Y. He, J. Hou, G. Yang and S. Zhou, *Small*, 2020, **16**, 1902262.
155 M. A. Subhan and M. M. Rahman, *Chem. Rec.*, 2022, **22**, e202100331.
156 P. B. da Silva, R. T. A. Machado, A. M. Pironi, R. C. Alves, P. R. de Araújo, A. C. Dragalzew, I. Dalberto and M. Chorilli, *Curr. Med. Chem.*, 2019, **26**, 2108–2146.
157 P. Liu, Z. Huang, Z. Chen, R. Xu, H. Wu, F. Zang, C. Wang and N. Gu, *Nanoscale*, 2013, **5**, 11829–11836.
158 M. Arumugam, B. Murugesan, N. Pandiyan, D. K. Chinnalagu, G. Rangasamy and S. Mahalingam, *Mater. Sci. Eng., C*, 2021, **123**, 112019.
159 S. Hofmann, C. T. Wong Po Foo, F. Rossetti, M. Textor, G. Vunjak-Novakovic, D. L. Kaplan, H. P. Merkle and L. Meinel, *J. Controlled Release*, 2006, **111**, 219–227.
160 A. L. Laiva, J. R. Venugopal, P. Karuppuswamy, B. Navaneethan, A. Gora and S. Ramakrishna, *Int. J. Pharm.*, 2015, **483**, 115–123.
161 G. J. Peters, *Nucleosides, Nucleotides Nucleic Acids*, 2014, **33**, 358–374.
162 E. Jaisankar, R. S. Azarudeen and M. Thirumarimurugan, *ACS Appl. Bio Mater.*, 2024, **7**, 4323–4338.
163 G. Kuang, Q. Zhang, Y. Yu, X. Ding, W. Sun, X. Shen and Y. Zhao, *Chem. Eng. J.*, 2023, **455**, 140619.
164 I. H. Abdulkareem and I. B. Zurmi, *Niger. J. Clin. Pract.*, 2012, **15**(1), 9–14.
165 K.-W. Kim, J. K. Roh, H.-J. Wee and C. Kim, in *Cancer Drug Discovery: Science and History*, ed. K.-W. Kim, J. K. Roh, H.-J. Wee and C. Kim, Springer Netherlands, Dordrecht, 2016, pp. 155–174.
166 P. de Medina, G. Favre and M. Poirot, *Anti-Cancer Agents Med. Chem.*, 2004, **4**(6), 491–508.
167 A. D. Pinzón-García, R. Sinisterra, M. Cortes, F. Mesa and S. Ramírez-Clavijo, *PeerJ*, 2021, **9**, e12124.
168 L. Ouyang, Y. Luo, M. Tian, S.-Y. Zhang, R. Lu, J.-H. Wang, R. Kasimu and X. Li, *Cell Proliferation*, 2014, **47**, 506–515.
169 J. Li, Q. Du, J. Wan, D.-G. Yu, F. Tan and X. Yang, *Mater. Des.*, 2024, **238**, 112657.

170 H. Chen, J. Wu, M. S. U. Rahman, S. Li, J. Wang, S. Li, Y. Wu, Y. Liu and S. Xu, *Biomater. Adv.*, 2023, **148**, 213358.
171 P. Famta, S. Shah, A. Sharma, G. Pandey, G. Vambhurkar, D. A. Srinivasarao, A. Asthana, B. K. Kumar and S. Srivastava, *J. Drug Delivery Sci. Technol.*, 2024, **99**, 105977.
172 S. T. Najjari, A. Asefnejad, P. G. S. Abadi, N. H. Nemati and M. Irani, *J. Polym. Environ.*, 2024, **32**, 791–802.
173 A. M. R. H. Mostafa, O. Petrai, A. A. Poot and J. Prakash, *Int. J. Pharm.*, 2024, **656**, 124078.
174 O. A. A. Alabrahim and H. M. E.-S. Azzazy, *Discover Nano*, 2024, **19**, 27.
175 K. Hasanbegloo, S. Banihashem, B. Faraji Dizaji, S. Bybordi, N. Farrokh-Eslamlou, P. G. Abadi, F. S. Jazi and M. Irani, *Int. J. Biol. Macromol.*, 2023, **230**, 123380.
176 J. Jaworska, R. Smolarczyk, M. Musiał-Kulik, T. Cichoń, P. Karpeta-Jarząbek, J. Włodarczyk, M. Stojko, H. Janeczek, A. Kordyka, B. Kaczmarczyk, M. Pastusiak and J. Kasperczyk, *Int. J. Pharm.*, 2021, **602**, 120596.
177 Z. Mohebian, M. Babazadeh, N. Zarghami and H. Mousazadeh, *J. Drug Delivery Sci. Technol.*, 2021, **61**, 102170.
178 Ş. M. Eskitoros-Togay, Y. E. Bulbul and N. Dilsiz, *Int. J. Pharm.*, 2020, **590**, 119933.
179 S. Rasouli, M. Montazeri, S. Mashayekhi, S. Sadeghi-Soureh, M. Dadashpour, H. Mousazadeh, A. Nobakht, N. Zarghami and Y. Pilehvar-Soltanahmadi, *J. Drug Delivery Sci. Technol.*, 2020, **55**, 101402.
180 X. Zhang, L. Han, Q. Sun, W. Xia, Q. Zhou, Z. Zhang and X. Song, *J. Biomater. Sci., Polym. Ed.*, 2020, **31**, 456–471.
181 P. Vashisth, M. Sharma, K. Nikhil, H. Singh, R. Panwar, P. A. Pruthi and V. Pruthi, *3 Biotech*, 2015, **5**, 303–315.
182 C. Xie, X. Li, X. Luo, Y. Yang, W. Cui, J. Zou and S. Zhou, *Int. J. Pharm.*, 2010, **391**, 55–64.
183 A. Hudecki, I. Rzeszutek, A. Lewińska, T. Warski, A. Baranowska-Korczyc, R. Wojnarowska-Nowak, G. Betlej, A. Deręgowska, J. Hudecki, D. Łyko-Morawska, W. Likus, A. Moskal, P. Krzemiński, M. Cieślak, M. Kęsik-Brodacka, A. Kolano-Burian and M. Wnuk, *Biomater. Adv.*, 2023, **153**, 213582.
184 P. B. Balakrishnan, L. Gardella, M. Forouharshad, T. Pellegrino and O. Monticelli, *Colloids Surf., B*, 2018, **161**, 488–496.
185 B. Darbasizadeh, S. A. Mortazavi, F. Kobarfard, M. R. Jaafari, A. Hashemi, H. Farhadnejad and B. Feyzi-barnaji, *J. Drug Delivery Sci. Technol.*, 2021, **64**, 102576.
186 H. Lian and Z. Meng, *Bioact. Mater.*, 2017, **2**, 96–100.
187 G. El Fawal, M. M. Abu-Serie, H. El-Gendi and E. M. El-Fakharany, *Int. J. Biol. Macromol.*, 2022, **204**, 555–564.
188 S. Banihashem, M. N. Nezhati, H. A. Panahi and A. Shakeri-Zadeh, *Int. J. Polym. Mater. Polym. Biomater.*, 2020, **69**, 1197–1208.
189 P. Dubey and P. Gopinath, *J. Mater. Chem. B*, 2016, **4**, 726–742.
190 J. A. Torres-Betancourt, R. Hernández-Delgadillo, J. V. Cauich-Rodríguez, D. A. Oliva-Rico, J. M. Solis-Soto, C. M. García-Cuellar, Y. Sánchez-Pérez, N. Pineda-Aguilar, S. Flores-Treviño, I. Meester, S. E. Nakagoshi-Cepeda, K. Arevalo-Niño, M. A. A. Nakagoshi-Cepeda and C. Cabral-Romero, *J. Funct. Biomater.*, 2024, **15**, 309.
191 E. Jaisankar, R. S. Azarudeen and M. Thirumarimurugan, *ACS Appl. Bio Mater.*, 2022, **5**, 4327–4341.
192 E. Jaisankar, R. S. Azarudeen and M. Thirumarimurugan, *J. Drug Delivery Sci. Technol.*, 2023, **84**, 104451.
193 N. K. Sedky, K. K. Arafa, M. M. M. Abdelhady, M. Y. Issa, N. M. Abdel-Kader, N. K. Mahdy, F. A. Mokhtar, M. Y. Alfaifi and S. A. Fahmy, *Pharmaceutics*, 2023, **15**, 2367.
194 S. Mozaffari, S. Seyedabadi and E. Alemzadeh, *J. Drug Delivery Sci. Technol.*, 2022, **67**, 102984.
195 H. Ataollahi and M. Larypoor, *Polym. Adv. Technol.*, 2022, **33**, 1468–1480.
196 R. Sedghi, M. Gholami, A. Shaabani, M. Saber and H. Niknejad, *Eur. Polym. J.*, 2020, **123**, 109421.
197 J. Xie, Z. Fan, Y. Li, Y. Zhang, F. Yu, G. Su, L. Xie and Z. Hou, *Int. J. Nanomed.*, 2018, **13**, 1381–1398.
198 J. Yan, Q. Wu, Z. Zhao, J. Wu, H. Ye, Q. Liang, Z. Zhou, M. Hou, X. Li, Y. Liu and L. Yin, *Biomaterials*, 2020, **255**, 120166.
199 L. Luo, Y. Qi, H. Zhong, S. Jiang, H. Zhang, H. Cai, Y. Wu, Z. Gu, Q. Gong and K. Luo, *Acta Pharm. Sin. B*, 2022, **12**, 424–436.
200 D. Schmaljohann, *Adv. Drug Delivery Rev.*, 2006, **58**, 1655–1670.
201 V. P. Torchilin, *Nat. Rev. Drug Discovery*, 2014, **13**, 813–827.
202 N. Mamidi, R. M. V. Delgadillo and J. V. Castrejón, *Environ. Sci.: Nano*, 2021, **8**, 2081–2097.
203 D. Liu, F. Yang, F. Xiong and N. Gu, *Theranostics*, 2016, **6**, 1306–1323.
204 W. Li, Y. Li, Z. Liu, N. Kerdsakundee, M. Zhang, F. Zhang, X. Liu, T. Bauleth-Ramos, W. Lian, E. Mäkilä, M. Kemell, Y. Ding, B. Sarmento, R. Wiwattanapatapee, J. Salonen, H. Zhang, J. T. Hirvonen, D. Liu, X. Deng and H. A. Santos, *Biomaterials*, 2018, **185**, 322–332.
205 Y. Tian, R. Tian, L. Chen, R. Jin, Y. Feng, Y. Bai and X. Chen, *Macromol. Rapid Commun.*, 2019, **40**, 1800824.
206 P. Nakielski, S. Pawłowska, C. Rinoldi, Y. Ziai, L. De Sio, O. Urbanek, K. Zembrzycki, M. Pruchniewski, M. Lanzi, E. Salatelli, A. Calogero, T. A. Kowalewski, A. L. Yarin and F. Pierini, *ACS Appl. Mater. Interfaces*, 2020, **12**, 54328–54342.
207 B. Wang, H. Zheng, M.-W. Chang, Z. Ahmad and J.-S. Li, *Colloids Surf., B*, 2016, **145**, 757–767.
208 H. Luo, K. Wu, Q. Wang, T. C. Zhang, H. Lu, H. Rong and Q. Fang, *J. Membr. Sci.*, 2020, **593**, 117406.
209 H. Ding, P. Tan, S. Fu, X. Tian, H. Zhang, X. Ma, Z. Gu and K. Luo, *J. Controlled Release*, 2022, **348**, 206–238.
210 E. K. Rofstad, B. Mathiesen, K. Kindem and K. Galappathi, *Cancer Res.*, 2006, **66**, 6699–6707.
211 S. Mehnath, K. Chitra, K. Karthikeyan and M. Jeyaraj, *Int. J. Pharm.*, 2020, **584**, 119412.

212 X. Zhu, Z. Yang, D. Gan, T. Cui, H. Luo, Y. Wan and Q. Zhang, *Appl. Mater. Today*, 2023, **31**, 101759.
213 A. Rakhshani, S. Maghsoudian, H. Motasadizadeh, Y. Fatahi, A. Malek-Khatabi, M. H. Ghahremani, F. Atyabi and R. Dinarvand, *J. Drug Delivery Sci. Technol.*, 2025, **104**, 106431.
214 F. Khatami, A. Baharian, S. Akbari-Birgani and N. Nikfarjam, *J. Drug Delivery Sci. Technol.*, 2023, **85**, 104606.
215 Y. Yang, K. Long, Y. Chu, H. Lu, W. Wang and C. Zhan, *Adv. Funct. Mater.*, 2024, **34**, 2402975.
216 T. L. Rapp and C. A. DeForest, *Adv. Drug Delivery Rev.*, 2021, **171**, 94–107.
217 M. S. Noh, S. Lee, H. Kang, J.-K. Yang, H. Lee, D. Hwang, J. W. Lee, S. Jeong, Y. Jang, B.-H. Jun, D. H. Jeong, S. K. Kim, Y.-S. Lee and M.-H. Cho, *Biomaterials*, 2015, **45**, 81–92.
218 J. Wang, Y. Liu, Y. Ma, C. Sun, W. Tao, Y. Wang, X. Yang and J. Wang, *Adv. Funct. Mater.*, 2016, **26**, 7516–7525.
219 D. Viswanath and Y.-Y. Won, *ACS Biomater. Sci. Eng.*, 2022, **8**, 3644–3658.
220 Y. Wu, M. R. K. Ali, B. Dong, T. Han, K. Chen, J. Chen, Y. Tang, N. Fang, F. Wang and M. A. El-Sayed, *ACS Nano*, 2018, **12**, 9279–9290.
221 M. Ren, J. Zhou, Z. Song, H. Mei, M. Zhou, Z. F. Fu, H. Han and L. Zhao, *Chem. Eng. J.*, 2021, **411**, 128557.
222 R. Jaswal, V. K. Kaliannagounder, D. Kumar, C. H. Park and C. S. Kim, *Composites, Part B*, 2022, **243**, 110129.
223 X. Wei, C. Liu, Z. Wang and Y. Luo, *Int. J. Pharm.*, 2020, **580**, 119219.
224 M. Sadeghi, F. Falahi, S. Akbari-Birgani and N. Nikfarjam, *ACS Appl. Polym. Mater.*, 2023, **5**, 2394–2407.
225 H. Chen, Y. Shi, L. Sun and S. Ni, *Life Sci.*, 2020, **258**, 118152.
226 X. Chen, R. Klingeler, M. Kath, A. A. El Gendy, K. Cendrowski, R. J. Kalenczuk and E. Borowiak-Palen, *ACS Appl. Mater. Interfaces*, 2012, **4**, 2303–2309.
227 Y. Yang, X. Liu, Y. Lv, T. S. Herng, X. Xu, W. Xia, T. Zhang, J. Fang, W. Xiao and J. Ding, *Adv. Funct. Mater.*, 2015, **25**, 812–820.
228 J. Zhang and R. D. K. Misra, *Acta Biomater.*, 2007, **3**, 838–850.
229 J. Estelrich, E. Escribano, J. Queralt and M. A. Busquets, *Int. J. Mol. Sci.*, 2015, **16**, 8070–8101.
230 K. E. Albinali, M. M. Zagho, Y. Deng and A. A. Elzatahry, *Int. J. Nanomed.*, 2019, **14**, 1707–1723.
231 H. Y. Son, J. H. Ryu, H. Lee and Y. S. Nam, *Macromol. Mater. Eng.*, 2013, **298**, 547–554.
232 L. Chen, A. Nabil, N. Fujisawa, E. Oe, K. Li and M. Ebara, *J. Controlled Release*, 2023, **363**, 550–561.
233 F. Serio, N. Silvestri, S. K. Avugadda, G. E. P. Nucci, S. Nitti, V. Onesto, F. Catalano, E. D'Amone, G. Gigli, L. L. del Mercato and T. Pellegrino, *J. Colloid Interface Sci.*, 2022, **607**, 34–44.
234 L. Chen, N. Fujisawa, M. Takanohashi, M. Najmina, K. Uto and M. Ebara, *Int. J. Mol. Sci.*, 2021, **22**, 2542.
235 G. Cirillo, U. G. Spizzirri, M. Curcio, S. Hampel, O. Vittorio, D. Restuccia, N. Picci and F. Iemma, *Mini-Rev. Med. Chem.*, 2016, **16**, 658–667.
236 Y. Qiu and K. Park, *Adv. Drug Delivery Rev.*, 2012, **64**, 49–60.
237 M. Karimi, A. Ghasemi, P. S. Zangabad, R. Rahighi, S. M. M. Basri, H. Mirshekari, M. Amiri, Z. S. Pishabad, A. Aslani, M. Bozorgomid, D. Ghosh, A. Beyzavi, A. Vaseghi, A. R. Aref, L. Haghani, S. Bahrami and M. R. Hamblin, *Chem. Soc. Rev.*, 2016, **45**, 1457–1501.
238 D. Samanta, N. Hosseini-Nassab and R. N. Zare, *Nanoscale*, 2016, **8**, 9310–9317.
239 J. Ge, E. Neofytou, T. J. I. Cahill, R. E. Beygui and R. N. Zare, *ACS Nano*, 2012, **6**, 227–233.
240 M. Zheng, S. Yao, Y. Zhao, X. Wan, Q. Hu, C. Tang, Z. Jiang, S. Wang, Z. Liu and L. Li, *ACS Appl. Mater. Interfaces*, 2023, **15**, 7855–7866.
241 A. Puiggalí-Jou, A. Cejudo, L. J. del Valle and C. Alemán, *ACS Appl. Bio Mater.*, 2018, **1**, 1594–1605.
242 R. Jia, L. Teng, L. Gao, T. Su, L. Fu, Z. Qiu and Y. Bi, *Int. J. Nanomed.*, 2021, **16**, 1525–1551.
243 A. P. Tiwari, T. I. Hwang, J.-M. Oh, B. Maharjan, S. Chun, B. S. Kim, M. K. Joshi, C. H. Park and C. S. Kim, *ACS Appl. Mater. Interfaces*, 2018, **10**, 20256–20270.
244 X. Zeng, M. Luo, G. Liu, X. Wang, W. Tao, Y. Lin, X. Ji, L. Nie and L. Mei, *Adv. Sci.*, 2018, **5**, 1800510.
245 S. A. A. Shah, M. Firlak, S. R. Berrow, N. R. Halcovitch, S. J. Baldock, B. M. Yousafzai, R. M. Hathout and J. G. Hardy, *Materials*, 2018, **11**, 1123.
246 L. Resina, F. F. F. Garrudo, C. Alemán, T. Esteves and F. C. Ferreira, *Biomater. Adv.*, 2024, **160**, 213830.
247 A. Martorana, G. Puleo, G. C. Miceli, F. Cancilla, M. Licciardi, G. Pitarresi, L. Tranchina, M. Marrale and F. S. Palumbo, *Int. J. Pharm.*, 2025, **669**, 125108.
248 S. Pirzadeh-Naeeni, M. R. Mozdianfard, S. A. Shojaosadati, A. C. Khorasani and T. Saleh, *Int. J. Biol. Macromol.*, 2020, **144**, 380–388.
249 Z. Yuan, W. Wu, Z. Zhang, Z. Sun, R. Cheng, G. Pan, X. Wang and W. Cui, *Colloids Surf., B*, 2017, **158**, 363–369.
250 R. Jaswal, D. Kumar, J. Lee, C. H. Park and K. H. Min, *Mater. Today Chem.*, 2024, **41**, 102294.
251 R. Jaswal, D. Kumar, A. I. Rezk, V. K. Kaliannagounder, C. H. Park and K. H. Min, *Colloids Surf., B*, 2024, **237**, 113820.
252 M. Cheng, H. Wang, Z. Zhang, N. Li, X. Fang and S. Xu, *ACS Appl. Mater. Interfaces*, 2014, **6**, 1569–1575.
253 Z. Zhang, S. Liu, H. Xiong, X. Jing, Z. Xie, X. Chen and Y. Huang, *Acta Biomater.*, 2015, **26**, 115–123.
254 N. Mauro, C. Scialabba, G. Pitarresi and G. Giammona, *Int. J. Pharm.*, 2017, **526**, 167–177.
255 S. Asgari, G. M. Ziarani, A. Badiei, A. Pourjavadi and M. Kiani, *J. Drug Delivery Sci. Technol.*, 2022, **76**, 103702.
256 A. GhavamiNejad, A. R. K. Sasikala, A. R. Unnithan, R. G. Thomas, Y. Y. Jeong, M. Vatankhah-Varnoosfaderani, F. J. Stadler, C. H. Park and C. S. Kim, *Adv. Funct. Mater.*, 2015, **25**, 2867–2875.

257 A. R. K. Sasikala, A. R. Unnithan, R. G. Thomas, S. W. Ko, Y. Y. Jeong, C. H. Park and C. S. Kim, *Adv. Funct. Mater.*, 2018, **28**, 1704793.
258 A. Farboudi, A. Nouri, S. Shirinzad, P. Sojoudi, S. Davaran, M. Akrami and M. Irani, *Int. J. Biol. Macromol.*, 2020, **150**, 1130–1140.
259 A. R. K. Sasikala, A. R. Unnithan, Y.-H. Yun, C. H. Park and C. S. Kim, *Acta Biomater.*, 2016, **31**, 122–133.
260 E. Niiyama, K. Uto, C. M. Lee, K. Sakura and M. Ebara, *Polymers*, 2018, **10**, 1018.
261 M. Abasalta, A. Asefnejad, M. T. Khorasani and A. R. Saadatabadi, *Carbohydr. Polym.*, 2021, **257**, 117631.
262 Q. N. Q. Vo, A. I. Rezk, S. Chun, C. H. Park and C. S. Kim, *Mater. Adv.*, 2024, **5**, 2128–2139.
263 S. Federico, A. Martorana, G. Pitarresi, F. S. Palumbo, C. Fiorica and G. Giammona, *Biomater. Adv.*, 2022, **136**, 212769.
264 D. Miao, Y. Song, S. De Munter, H. Xiao, B. Vandekerckhove, S. C. De Smedt, C. Huang, K. Braeckmans and R. Xiong, *Nat. Protoc.*, 2025, **20**, 1810–1845.
265 N. Mamidi and A. O. Mahmoudsalehi, *J. Mater. Chem. B*, 2025, **13**, 10440–10459.
266 T. Yamashita, S. Saji, T. Takano, Y. Naito, M. Tsuneizumi, A. Yoshimura, M. Takahashi, J. Tsurutani, T. Iwatani, M. Kitada, H. Tada, N. Mori, T. Higuchi, T. Iwasa, K. Araki, K. Koizumi, H. Hasegawa, Y. Uchida, S. Morita and N. Masuda, *J. Clin. Oncol.*, 2025, **43**, 1302–1313.
267 M. Du, S. Liu, N. Lan, R. Liang, S. Liang, M. Lan, D. Feng, L. Zheng, Q. Wei and K. Ma, *Regener. Biomater.*, 2024, **11**, rbad114.
268 J. Zhao and W. Cui, *Adv. Fiber Mater.*, 2020, **2**, 229–245.
269 K. You, Q. Wang, M. S. Osman, D. Kim, Q. Li, C. Feng, L. Wang and K. Yang, *BMEMat*, 2024, **2**, e12067.
270 X. Yang, Q. Wang, Z. Zhu, Y. Lu, H. Liu, D.-G. Yu and S.-W. A. Bligh, *Pharmaceutics*, 2025, **17**, 1152.
271 H. Lv, P. Wang, Y. Lv, L. Dong, L. Li, M. Xu, L. Fu, B. Yue and D. Yu, *Catalysts*, 2025, **15**, 163.
272 P. Wang, Y. Liu, W. He, Y. Chen, J. Zhou and D.-G. Yu, *Adv. Mater. Interfaces*, 2025, **12**, e00364.
273 D.-G. Yu, W. He, C. He, H. Liu and H. Yang, *Nanomedicine*, 2025, **20**, 271–278.
274 Y. Hu, F. Zhang, J. Zhou, Y. Yang, D. Ding, M. Li, C. Wang, B. Wang, J. Yu, F. Jiang, D.-G. Yu and H. Shen, *Small*, 2025, e05523, DOI: 10.1002/smll.202505523.
275 D.-G. Yu and J. Zhou, *Next Mater.*, 2024, **2**, 100119.
276 Y.-S. Zhao, J. Huang, X. Yang, W. Wang, D.-G. Yu, H. He, P. Liu and K. Du, *Front. Bioeng. Biotechnol.*, 2025, **13**, DOI: 10.3389/fbioe.2025.1533367.
277 W. Wang, X. Yang, H. Yin, Y. Lu, H. Dou, Y. Liu and D.-G. Yu, *Macromol. Rapid Commun.*, 2025, **46**, 2401152.
278 S. Zhang, W. Yang, W. Gong, Y. Lu, D.-G. Yu and P. Liu, *RSC Adv.*, 2024, **14**, 14374–14391.
279 W. Gong, M.-L. Wang, Y. Liu, D.-G. Yu and S. W. A. Bligh, *Int. J. Mol. Sci.*, 2024, **25**, 9556.
280 R. Dong, W. Gong, Q. Guo, H. Liu and D.-G. Yu, *Polymers*, 2024, **16**, 2614.
281 Y. Chen, W. Gong, Z. Zhang, J. Zhou, D.-G. Yu and T. Yi, *Int. J. Mol. Sci.*, 2024, **25**, 9524.
282 J. Kim, Y. H. Hwang, G.-H. Nam and I.-S. Kim, *J. Controlled Release*, 2026, **389**, 114462.
283 Y. Fang, X. Luo, Y. Xu, Z. Liu, R. L. Mintz, H. Yu, X. Yu, K. Li, E. Ju, H. Wang, Z. Tang, Y. Tao and M. Li, *Adv. Sci.*, 2023, **10**, 2300899.
284 Y. Fang, Z. Liu, H. Wang, X. Luo, Y. Xu, H. F. Chan, S. Lv, Y. Tao and M. Li, *ACS Appl. Mater. Interfaces*, 2022, **14**, 27525–27537.
285 K. Li, X. Yu, Y. Xu, H. Wang, Z. Liu, C. Wu, X. Luo, J. Xu, Y. Fang, E. Ju, S. Lv, H. F. Chan, Y.-H. Lao, W. He, Y. Tao and M. Li, *Nat. Commun.*, 2025, **16**, 1629.